- Modelling of Magnetic Aggregation of Stem Cells in Microfluidics -

- Shaikh Sohail Faizan Nisar Ahmed -

A Dissertation Submitted to

Indian Institute of Technology Hyderabad

In Partial Fulfillment of the Requirements for

The Degree of Master of Technology

भारतीय प्रौद्योगिकी संस्थान हैदराबाद
Indian Institute of Technology Hyderabad

Department of Biomedical Engineering

June, 2015

Declaration

I declare that this written submission represents my ideas in my own words, and where others' ideas or words have been included, I have adequately cited and referenced the original sources. I also declare that I have adhered to all principles of academic honesty and integrity and have not misrepresented or fabricated or falsified any idea/data/fact/source in my submission. I understand that any violation of the above will be a cause for disciplinary action by the Institute and can also evoke penal action from the sources that have thus not been properly cited, or from whom proper permission has not been taken when needed.

_____

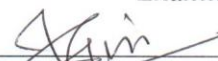(Signature)

_____

(Shaikh Sohail Faizan)

_____

(BM13M1005)

ii

Approval Sheet

This thesis entitled – Modelling of Magnetic Aggregation of Stem Cells in Microfluidics – by – Shaikh Sohail Faizan – is approved for the degree of Master of Technology from IIT Hyderabad.

-Name and affiliation-

Examiner

Dr Jyotsnendu Giri

Assistant Professor, Department of Biomedical Engineering,

Indian Institute of Technology Hyderabad

Examiner

Dr Harikrishnan Narayanan Unni

Assistant Professor, Department of Biomedical Engineering,
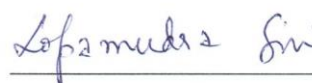
Indian Institute of Technology Hyderabad

Advisor

Dr Subha Narayan Rath

Assistant Professor, Department of Biomedical Engineering,

Indian Institute of Technology Hyderabad

Co-Advisor

Dr Lopamudra Giri

Assistant Professor, Department of Chemical Engineering,

Indian Institute of Technology Hyderabad

Chairman

Acknowledgements

Dedicated to

My family and relatives

Abstract

Individual cells assemble to form multi-cellular aggregates in a hierarchical manner over different length scales to coordinate the tissue functions. Current approaches to control the assembly and patterning of stem cells in 3D, require intrinsic adhesive properties, chemical modifications of cell and material interfaces or engineering intracellular interactions. A particular concern in surface modification of stem cell for adhesion properties, is the possibility of attenuation and inhibition of signalling pathways critical for differentiation of cells. Microfabrication technologies enable extremely fine-tuned culture management by means of control and reproducibility of extracellular stimulus (cues) to the levels unachievable by traditional standard tissue culture. Recent advances in microfabrication technologies and studies in microfluidics demonstrate the usage of magnetic forces that can be broadly applied across multiple length scales to direct individual cells for aggregation at microscales, and have long been used for large scale applications such as sorting and separating population of cells. Recent experiments suggest that magnetic microparticles (magMPs) can be efficiently incorporated in dose-dependent manner in extra-cellular environment of stem cells without any chemical and surface modifications of stem cells and assembly.

In this study we propose a sophisticated model of a microfluidic device for EB formation and spatial patterning on-chip by micropatterning of thick neodymium iron boron (NdFeB) magnetic film (20-100µm) on a glass substrate. It is important to know the field distributions and forces acting on the cells flowing in the microfluidic channel, and variations in different patterns. For this purpose, numerical finite element simulations are performed using COMSOL multiphysics. Small magnets permit very precise control of the magnetic field and when positioned in close proximity of microchannel, field strength requirements are reduced. This approach is expected to provide new routes to study differentiation of stem cells that will be helpful in addressing the critical questions in scaffold-free tissue engineering, developmental biology and regenerative medicine.

Contents

Chapter 1

Introduction

Mammalian tissues are comprised of hierarchically assembled cellular units to contribute for a specific tissue function and organ. Engineering tissues *in vitro* requires mimicking the complex environment of organs and native tissues by creating 3D multi-cellular aggregates capable of serving as models for healthy and diseased tissues, for use as novel diagnostic and drug-screening platforms[1] in organ replacement and regenerative therapies. Stem cells bear a great therapeutic potential in tissue engineering and regenerative medicine owing to their unlimited proliferative and differentiation capabilities[2]. Most commonly followed protocol for inducing differentiation rely on cell aggregation and formation of 3D colonies known as embryoid bodies (EBs)[3]. This method of inducing differentiation closely mimics the embryonic development process. During initial few days of differentiation, EBs produce the population of embryonic primitive cell lineages while over an extended duration of culture, neuronal, hematopoietic and muscle cells can be detected. EB size and shape has also been reported for playing critical role in the differentiation fate[4-5].

This thesis explores the model for using microfabricated magnets patterned on the glass surface to aggregate and manipulate stem cells for differentiation studies. This study is seemed to be useful in addressing challenging questions in the field of developmental biology, stem cell research and tissue engineering. This chapter deals with the overview of fundamental information about stem cells, need of the advanced technology for stem cell research, microfluidics, lab-on-a-chip devices and integration of sensory systems.

1.1   What are Stem Cells?

In a multicellular organisms, cells constantly communicate with each other in environment rather than existing in isolation. Mammalian tissues are comprised of individual cells that assembles in a hierarchical manner to form multicellular units[6]. These units span over differential length scales to coordinate and contribute to a particular tissue function and organ. Stem cells are foundation blocks of each and every organ and tissue in

our body. Tissues are made up of highly specialized cells which originally come from initial pool of stem cells, formed shortly after fertilization. Through out of life, we rely on stem cells that serve as the repair system for the body, replace injured tissues, and cells that are lost every day, such as in our skin, hair and blood etc. Theoretically, they can divide without limit to replenish other cells as long as a person or animal is alive.

Stem cells have two important characteristics that distinguish them from other specialized types of cells. First, they are unspecialized cells having capability of self-renewing for long periods through self-division. The second is, under certain physiological or experimental conditions they can differentiate into specialized cells that are mature and make up our organs and tissues[7]. Researchers work primarily with two kinds of stem cells from animals and humans: Embryonic stem cells and adult (tissue specific) stem cells:

Tissue specific stem cells, also referred as somatic stem cells are somewhat specialized to produce few or all cell types found within a particular tissue or organ in which they reside. They are also termed as multipotent for their ability to generate multiple, organ-specific cell types. They are found in several organs that need continuous replacement like blood, skin, hair, and gut. They are also found in brain cells.

Embryonic stem cells (ESCs) are termed as pluripotent which means they are capable of generating all types of cells in the body. ESCs are obtained from the blastocysts — a very early stage of embryo which is 3 to 5 days old that consists of only 150-200 cells.

It has been hypothesized by scientists, that stem cells in future will become the basis for treating the neurodegenerative diseases such as Parkinson's disease, Alzheimer's disease, heart diseases etc.[8]. Scientists are studying stem cells in the laboratory to learn about their essential properties and what makes them different from specialized cell types. This fundamental understanding can lead to the usage of cells not only in cell based therapies but also for screening new drugs, toxins, and understanding the birth defects. Hence, researchers are intensively studying properties of stem cells that include:

- Determining precisely, how stem cells remain unspecialized without differentiation and proliferate, self-renew for a year or a longer period?

- Identifying the factors and understanding the signaling that induce differentiation[8].

1.2   Need for Advanced Technology in Stem Cell Research

Due to the unlimited proliferation and differentiation capabilities, stem cells bear a great therapeutic potential in regenerative medicine and tissue engineering. In 2010, the global stem cell market was estimated at $21.5 billion and was projected to reach $63.8 by the end of 2015[9]. This outlines the importance of stem cell technology for medical

therapeutic, drug development, and a variety of healthcare application like toxicological studies, disease modelling and cell replacement therapies.

Stem cells offer consistent supply of relevant cells from pathogen free sources that can differentiate into somatic cells, *in vivo* and *in vitro*. These have been successfully used to replace lost cells due to degenerative diseases and also assist in damaged tissue repair. An important aspect of stem cell research is the availability of well characterized and validated pluripotent stem cells similar to the renowned cell banks. Consequently, the major challenges in culturing stem cells *in vitro* are: expansion control while maintaining homogenous undifferentiated cells, and the ability to control and direct the differentiation reliability. Different conventional methods are in practice for cell-assays, however, their drawbacks include limited reliability, reproducibility and robustness, which may lead to experimental inconsistencies and difficulties in cell culture propagation and differentiation. Additionally, end point detection methods based on optical labels gives limited view on dynamic cellular mechanism.

Lab-on-a-chip (LOC) technology could deliver the next generation cell analysis tool capable of inexpensively testing large number of cells or small number of cell population under great control and reproducible conditions[10]. Microfluidic systems play a vital role in stem cell research, since these are the only technology capable of providing spatial and temporal control over cell growth and stimuli, by combining surfaces that mimics complex biochemistry and extracellular matrix (ECM) geometries with fluidic channels to regulate transport of fluid and soluble factors.

1.3 Microfluidics for Cell Culture

Microfluidics emerged as an extension of microelectro-mechanical systems (MEMS) technology at the beginning of 1980s. Microfluidics deals with the fluid (in µl) in channels in micrometer range, typically 10-100µm and has applications in the fields of engineering, chemistry and biotechnology etc. Advantages of microfluidics due to its smaller size includes- reduced reaction rate & analysis time, reduced consumption of reagents, reduced production of potentially harmful byproducts, and possibility to run multiple assays or multiple integrated processes on a single chip[11]. Flows in microfluidics systems show laminar behavior that implies- the flow can only be mixed by diffusion or active mixing by applying different forces. This provides the great control over the concentration of molecules or analytes in space and time, and simplifies the analysis of fluid or molecules due to well defined behavior. The concentration or aggregation of stem cells is

important in the formation of embryoid bodies (EBs) - crucial in inducing differentiation of stem cells.

Microfluidic devices are heart of the development of analytical systems, biomedical devices, tools for chemistry and biochemistry, and fundamental research in biology. These are often termed as micro-total analysis systems (µTAS) or LOC devices that integrates reacting chambers, sensors and fluid control on chip. These devices act as perfect platform to study cells under various specific microenvironmental conditions[12]. The fluid flow generated exhibits some features relevant to the fluid in biological systems such as high surface to volume ratio and maintaining a control microenvironment.

Miniaturization of cell-culture platforms allow us to observe the cellular behavior and interaction at the scale found in living systems. Microtechnology and microfluidics provide the means to engineer the cell-culture platforms that resemble closely *in vivo* than conventional dish cultures. Microfluidic devices that mimic vasculature *in vivo*, are excellent platforms for studying the cellular perfusion and can also act as powerful tools to control the parameters of cell-culture environment[11]. Taking a step further, these devices are extensively used in stem cells and biomedical research to achieve the microenvironment condition control and its mimicking to the level that is highly impossible to achieve through convention dish culture. The cell microenvironment is of the most importance in stem cell differentiation. Also, the transparent nature of devices allows the real time monitoring and analysis of the stem cell behavior with the integration of high resolution imaging technologies.

Different studies and aspects of LOC devices are mentioned here. This includes the applications and technologies for trapping, selecting and sorting of cells. This implies the identification, separation and positioning of desired cell types within LOC system using existing techniques of geometric traps, gravitational fluid flow fractionation, Dielectrophoresis (DEP), and optical tweezers etc. The shape and size of stem cell EBs play an important role in its differentiation and determine the fate of the cells. This leads to the research and applications of LOC for patterning of the cells that separates cultivation and fluid handling areas within LOC device along with spatially defining co-culture models to study differentiation and signaling mechanism.

Advancement in microfabrication technologies and LOC research has enabled creation of increasingly complex devices that includes valves and micropumps, on- chip biosensors, mixers, and degassers as well as multiple array of wells and chambers for multiplexed simultaneous analysis of cells[11]. The chemical gradient and soluble factors in the environment and culture condition play vital role in cell growth. This proof of concept

also applies to the stem cell and has been under research for several years. The potential benefits of the microfluidics gradient are highlighted in the recent publications. The microfluidic gradient generators have been used in stem cell culture to investigate the effect of growth factors and chemotaxis on stem cell differentiation within a single LOC device.

Besides being influenced by biochemical, structural, and environmental cues stem cell fate is also strongly effected by mechanical stress, electromagnetic forces, and acoustic and ultrasound stimulation. This ability of LOC systems to reproduce defined stimulations allows reliable investigation of cell behavior in an environment that mimics the mechanical forces within a living system. The importance of mechanical strain on fostering the stem cell differentiation *in vitro* has been shown into osteogenic, chondreogenic, smooth muscles and endothelial lineages[11].

1.4   Integration of Sensory Systems

A major advantage of lab-on-a-chip technology resides its portability, reliability, reproducibility, cost effectiveness and multiplexing different reactions in a single chip is that it facilitates integration of the electrical, optical, magnetic and acoustic sensors into the same chip. However most common used and preferred method of end point analysis is optical immune-fluorescence method. In almost all applications label free optical imaging of stem cells surface proteins is accomplished using Surface Plasmon Resonance (SPR).

Different electro-analytical methods are used in order to determine the electrical properties of stem cells such as voltammetry, potentiometry and impedance spectrometry to extract the information about cell viability, proliferation and differentiation. A commonly used electro analytical method to stimulate and analyze electrically active cells such as muscle cells is potentiometry which measures the changes in potential at two nodes because of the certain cellular activity. Moreover microelectrode arrays (MEAs) have been used to analyze electrical conductivity to investigate the ability of regenerating the damaged heart tissues after Ischemia or Infraction impedance spectrometry is another powerful, non-invasive and label free electro analytical method to assess the cell morphological changes migration, stress responses and differentiation.

Dielectrophoresis is another label free and non-invasive technique used for cell sorting, trapping, patterning and concentrating, and is also used to understand stem cell differentiation. This integration of sensory systems with LOC is explained in the following paragraphs with examples of different techniques in a particular application including cell manipulation, sorting and handling. These methods are categorized based on the physical

forces employed into-magnetic, optical, electrical, mechanical and acoustic manipulation of cells.

1.4.1 Hydrodynamic/ Mechanical Trapping

The most common way of realizing cell or particle trapping function in LOC devices the creation of side channels in a main channel for suction when a friction of total flow is aspirated, and the creation of different physical geometries within channel for physical entrapment. This physical entrapment method is useful in both single cell as well as cell aggregates depending upon the size of traps. Thus, array based approach for hydrodynamic trapping similar to that of microwell array cell traps was introduced by Zheng et al. who used reactive ion etching to form an array of circular through holes in a film[13]. Holes size was defined to capture the circulating tumor cells (CTC) and allow erythrocytes to pass through membrane. About 80% of CTC were captured in the membrane using this technique.

Approaches to format the arrays for single cell trapping has also been reported by Lee's group, who designed a hydrodynamic trapping array where trapping posts were arranged in a slanting position in flow through the chamber, shown in Fig. 1.1. Each post was designed to accommodate only a single cell or a small group of cells[14]. This trapping approach was modified further by Voldman's group who not only offered single cell trapping but also enabled cell pairing[15]. The hydrodynamic cell trapping is achieved by providing the trapping post with a deeper recess at the backside of the first post which in forward flow traps the single cell, depicted in Fig. 1.2. As the flow is reversed, cell is transferred into backside deeper recess and soon the second cell type is introduced in the same flow to capture and pair.

Due to the complex physical properties of cells, mechanical manipulation of cells on-chip poses certain challenges. Separation of targeted cells is the main application of mechanical manipulation that can be achieved by fabrication of constricted structures such as microfilters, microwells, dam structure, sandbag structures or modifying the microchannel inner surface with the reactive coating with antibodies and with enzymes etc. Size dependent filter based microfluidic devices have several advantages of high labelling efficiency, short detection time, high reproducibility, and high detection sensitivity at a whole level. On the other hand, the applications are limited due to poor selectivity. In some cases complicated fabrication procedure makes it difficult to use in common biological applications.
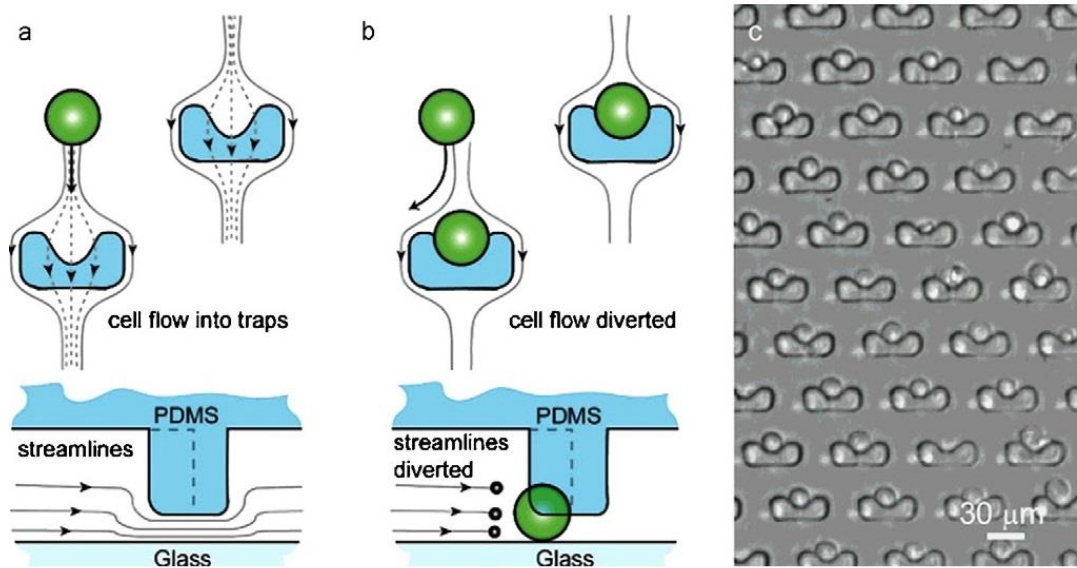
Figure 2.1.1 Hydrodynamic cell trapping array demonstrated by Di Carlo et al.
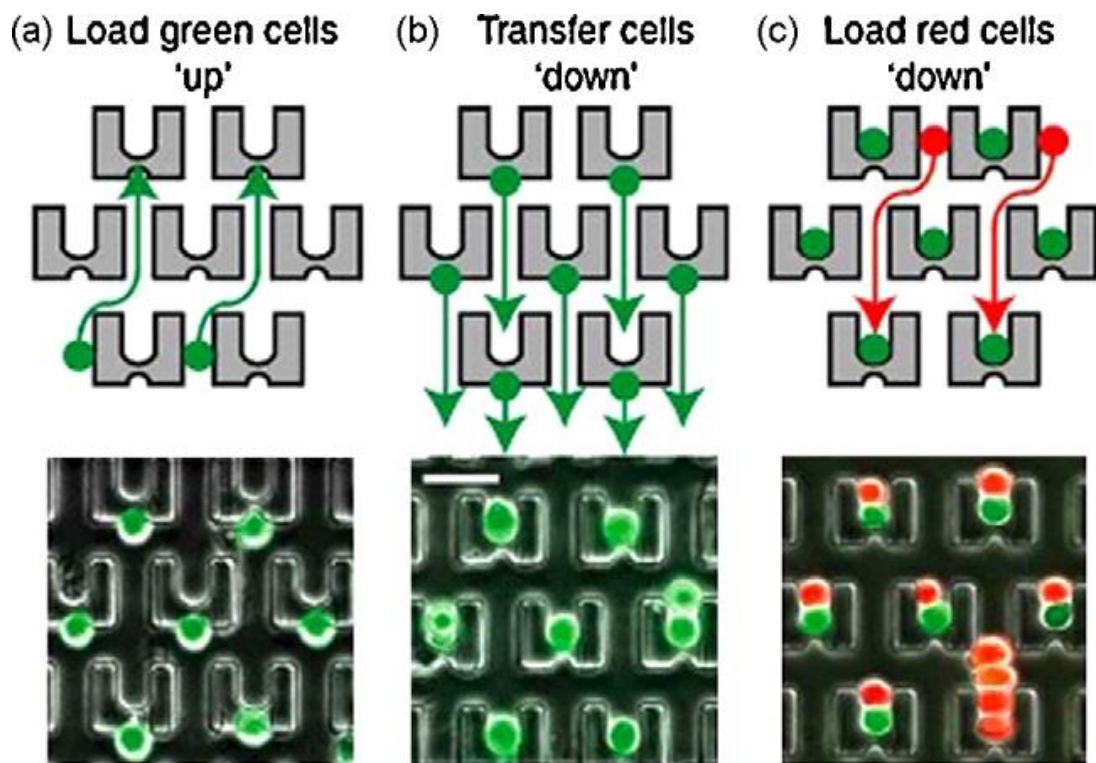

Figure 1.2 Hydrodynamic single cell pairing reported by Skelley et al.

1.4.2 Electrical Methods of Manipulation

Different electrical methods used in microfluidic applications comprise of electro-osmosis, electrophoresis and dielectrophoresis (DEP). In electroosmotic flow, an electrical

double layer (EDL) is induced at charge surface in contact with liquid due to charge separation. One charge is immobilized while other is free to move within the fluid. An external field parallel to the flow can drag the liquid in same direction, as the charges migrate in a manner similar to the electrophoresis due to shear force. Electroosmotic flow is well established in microfluidics for wide range of applications owing to the ability of changing directions of flow by changing the driving electrical field.

In electrophoresis, charged particles experience the electrostatic force and they migrate with a fixed velocity that depends on the polarity, mobility, size of the particle and viscosity of the medium. This is mainly used for the movement of charged particles in the uniform electrical field.

DEP is the movement of dielectric object because of electrical force generated by non-uniform electric field. It can also be defined as the lateral motion imparted in uncharged particles as a result of polarization from a non-uniform electrical field. DEP was first described and coined by Pohl in 1951 and thoroughly described by 1978[16].

A dielectric object with a permittivity different from the medium, surrounded by a non-uniform varying electric field experiences a net force that is given by:

$$F_{DEP} = 2\pi\varepsilon_m a^3 \, \mathrm{Re}(\mathrm{f}_{CM})\nabla\left|E^2\right| \qquad (1.1)$$

where, a is the radius of object, E is root mean square of electric field, f_{CM} is Clausis-Mossotti's factor which is determined by complex permittivities that are function of conductivity (σ), frequency (ω) of the field and permittivity (ε).

$$\mathrm{f}_{CM} = \frac{\varepsilon_p^* - \varepsilon_m^*}{\varepsilon_p^* + 2\varepsilon_m^*} \qquad \text{where, } \varepsilon^* = \varepsilon - j\frac{\sigma}{\omega} \qquad (1.2) \,\&\, (1.3)$$

Where, ε_p^* and ε_m^* are the complex permittivities of particle and medium respectively.

From above equations, we can observe that, when $\mathrm{f}_{CM} > 0$, then objects experiences a positive dielectric force (p-DEP) resulting in a movement towards high electric field. If $\mathrm{f}_{CM} < 0$, then the resulting negative dielectric force (n-DEP) cause the object movement away from high electric field.

In last two decades, DEP has found tremendous applications due to MEMS technology that allows fabrication of complex, high field at low voltage electrode arrays. The applications of DEP in microfluidics can be divided in subgroups for cell trapping and handling as-

-DEP attraction that uses p-DEP to concentrate and collect particles at a particular location in LOC device.

-DEP deflection that uses n-DEP force for repelling particle away from electrode edges in a highly conductive medium.

-Travelling wave DEP (TwDEP) which utilizes the electrode pair combination to create particle repellent zones. When the electrode pairs are activated alternatively, the particles can be moved in peristallic fashion even in non-flow situations.

Electrodeless pDEP trapping and nDEP deflecting are other categories.

1.4.3   Acoustic Manipulation

When a channel containing liquid and particles is excited acoustically at particular frequencies, then ultrasound standing waves (i.e. surface acoustic wave (SAW)) with induced nodes and anti-nodes are formed[16]. These sites are mostly occupied by particles, since they represent energetic minima. Thus, ultrasonic SAW can be used for non-contact cell trapping, manipulation and handling. Acoustic trapping is easily facilitated in microfluidic and hence, have predominant applications in cell handling and trapping in cell studies, biosensors etc.

SAW generates a pressure gradient which in a liquid medium exerts a force on particles having distinguished density and compressibility compared to the medium. Acoustic force experienced by the particles can be given by the following equations:

$$F_{acoustic} = \frac{P^2 \pi V_p \beta_m}{2\lambda} \phi \sin(\tfrac{4\pi x}{\lambda}) \tag{1.4}$$

Where, P is pressure amplitude, V_p is the volume of particle, β_m is the medium compressibility, λ is the acoustic wavelength and ϕ represent acoustic contrast factor.

$$\phi = \frac{\rho_p - \rho_m}{2\rho_p + \rho_m} - \frac{\beta_p}{\beta_m} \tag{1.5}$$

Where, ρ_p and ρ_m are densities of particle and medium respectively, β_p is the compressibility of the particle.

ϕ Determines whether the force is directed towards the pressure nodes or anti nodes. However, in typical trapping of cells, the force is directed towards the pressure nodes of a wave.

1.4.4   Optical Manipulation

Another contactless approach for trapping and handling the microparticles or cells is using the optical forces. Microobjects can be held in the region of a laser beam by negative light pressure. Particle can be dragged with the light spot and placed on the x-y plane when the beam is laterally moved. Additionally, if condensed light beams are used then the particle position in z-direction can also be controlled. Hence, optical tweezers give many applications in biology but are expensive. This process is getting more interest due to contamination free and contactless nature of manipulation. High resolution optical tweezers can also be used for single cell trapping and analysis, but they have limited manipulation area because of tight focusing requirements. They provide better spatial resolution but are expensive and have most complicated setups.

1.4.5   Magnetic Methods of Manipulation

Magnetic trapping, handling and sorting utilizes the magnetic fields and magnetic microparticles (magMP) of different parameters. Typical magMP have magnetic core and a non-magnetic coating that is often attached to antibodies. This method of selectively attaching magMP to specific cells and labelling of antibodies is commonly practiced for cell separation and purification in microfluidics. Usually, the size of MP and super-paramagnetic beads that are used in these applications varies between 10 nm to a few μm, but mostly 10 - 100 nm. This extremely small diametric particles give the advantage of not affecting the cell viability and cellular functions. These devices have high specificity and efficiency that make them most useful for obtaining rare cell types especially in handling red blood cells (RBCs)[17].

The magnetic forces experienced by particles can be expressed as function of particle volume V, magnetic susceptibility difference between medium and particle ($\Delta\chi$), and the strength and gradient of the applied magnetic field (B).

$$F_m = \frac{V(\Delta\chi)}{\mu_0}(\overline{B}\cdot\nabla)\overline{B} \tag{1.6}$$

$$\Delta\chi = \chi_p - \chi_m$$

Magnetic force will not act on particle in a homogenous field due to zero magnetic gradient. The typical values of magnetic force experienced by particles are found to carry from few pN to tens of pN and in some exceptional case to 100s of pN.

Magnetic trapping and handling of cells utilizes two types of magnets for realization: First, is the traditional permanent magnets and the second is usage of electromagnets. Permanent magnets are very common and still in practice due to the fact that they exert a large force on particles compared to electromagnets. An example in this case is demonstrated by Gijs et al., exerting about 40pN on 500nm particles when using a 5mm permanent magnet, while an electromagnet would exert 100 times lower force[18]. Magnetic methods have several advantages over different methods such as they are not affected by the surface charges, pH, ionic concentration or temperature[19].

Some of the strongest magnetic fields can be achieved using Samarium-Cobalt (SmCo) or Neodymium-Iron-Boron (NdFeB). The permanent magnets used in common application are small NdFeB magnets that features magnetic flux densities of up to 500mT which allows the manipulation of magMP inside channels even when magnet is placed at a distance of several millimeters from channel. Electromagnets can be switched on and off unlike permanent magnets, however, it is difficult to get the desired high field even when using large number of windings and high currents. Furthermore, heating effects could dominate and damage the device as well as have negative effects on cell viability.

Though, magnetic forces die rapidly as distance increases, it is a wide range force compared to the electrical forces that dies off within a few micrometer scales shown in Fig. 1.3. The requirement of high magnetic fields can be reduced by microfabricating the magnets in closed proximity to the channel using advanced microfabrication technologies. This fabrication involves considerable number of steps but they provide precise control over the magnetic field[19].

Overall considering the advantages and disadvantages of different techniques whether they are electrical, optical, mechanical, acoustic or magnetic, magnetic methods have dominant advantages. These include- wide range forces, negligible effect on cell viability, are not affected by properties of medium such as pH, temperature, ionic concentration etc. These provides larger surface area, clean versatile and non-invasive method that are stably controlled. Considering these advantage with the advancements in microfabrication technologies for patterning of magnets, and the new generation of magnetic beads materials it is foreseen that magnetic manipulation methods will be more efficient and easily integrated into microfluidic based cell assays as studied and demonstrated by our work.
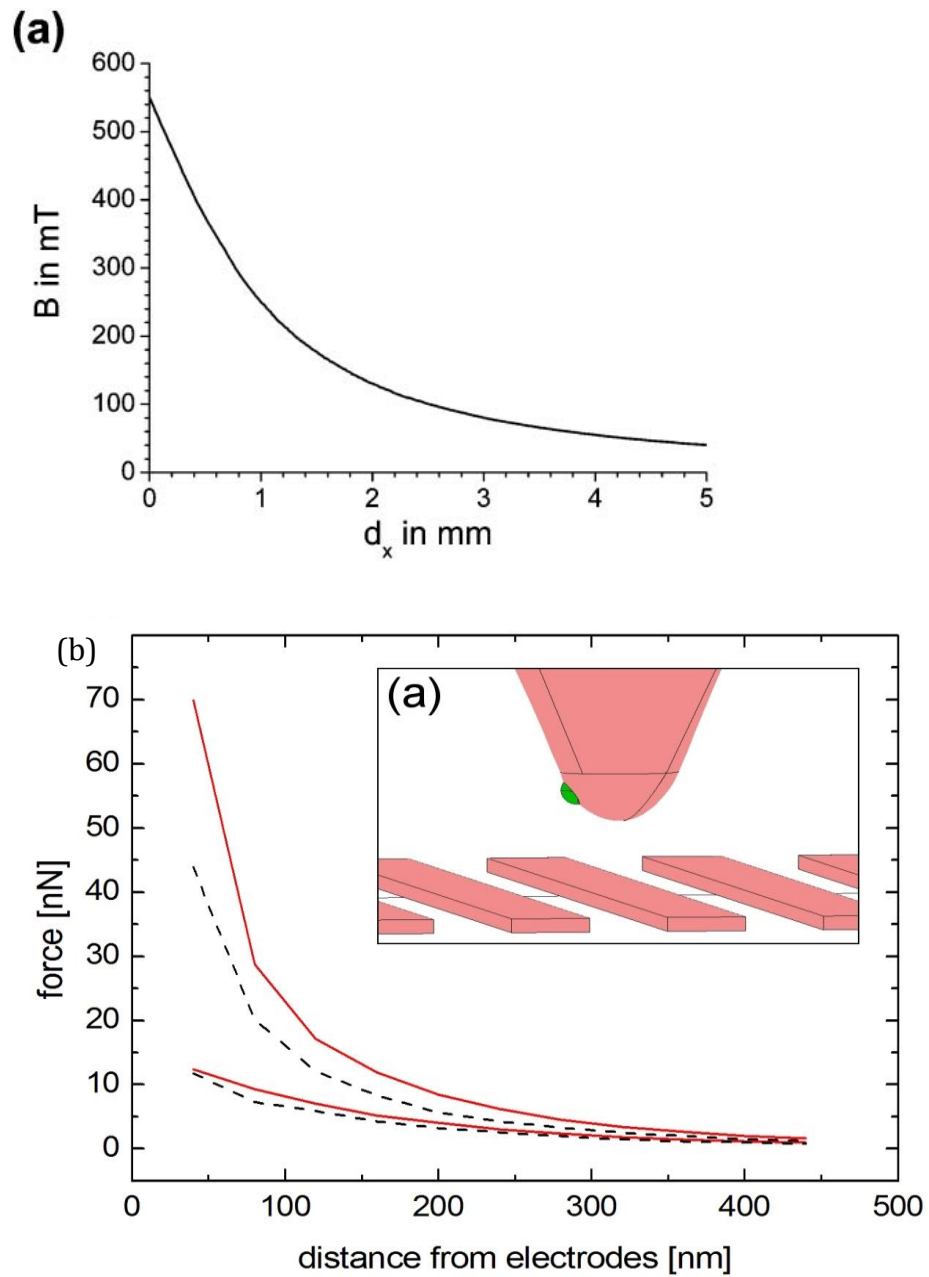
Figure 1.3 Comparison of magnetic and electrical field ranges a) magnetic field last for few mm (Pamme et al.) while b) electrical field dies off rapidly within few hundred nm even when high field is generated using sharp electrode (Jenke et al.)

Chapter 2

Previous Studies

First chapter of introduction has explored the fundamentals of the basic technologies used for cell handling and manipulation. This chapter explores the different studies carried out across the scientific community on stem cell differentiation or manipulation, patterning and applying magnetic methods for addressing the challenges in the field and their scope in future direction. It also provides details of different magnetic methods for these studies. At the end of this chapter we would be able to recognize the exact need of the work presented and will give the overall picture of the study performed by us.

2.1   Program Assembly of 3-Dimension Microtissues With Defined Cellular Connectivity

Multicellular organs are composed of basic units called cells which are differentiated into specialized and interdependent functions. Their spatial arrangement and connectivity is important for properly contributing to a specific tissue or organ function[20]. This cells live and communicate in the microenvironment by exchange of electrical, chemical and contact dependent signals. The unique microenvironment which have different and crucial effects on the control of cellular cycle, migration and differentiation of cell is defined by the convergence of these communicating signals. For example, contact dependent signals between cells give deterministic information about the short range structures and tissue behavior. Specific contacts between stem cell and surrounding microenvironment (stroma) are vital for organization and maintenance of adult stem cell niches from diverse tissue and organisms.

Mimicking the cell-cell interaction *ex vivo* remains an important challenge for the engineers, whether the application in building materials for tissue repair *in vivo* or *in vitro* realistic tissue model construction. The ability to control the inter connectivity among cells in surrounding has yet to be acquired despite extensive research progress has been made towards defining the cellular and ECM interactions[21]. 2-D cellular arrays of multiple cell

types have been produced by strategies like layer by layer printing, directed assembly using DEP forces or lasers, and a variety of photolithographic techniques[22-24]. On the other hand, these methods may not be suitable enough easily for generation of control inter connected 3D multicellular structures.

Gartner et al. developed a bottom-up approach to the construction of microtissues with specified connectivity by step wise formation of contacts between individual cells. The two main requirements were: the two cells with mutual reactivity and the ability to separate or filter out the multicellular products from unreacted individual cells. The group has reported a method of functionalizing the cell surfaces with the purpose of cell patterning on complementary DNA coated surface. They also investigated that the assembly of cell-cell contact can be directed by hybridization between DNA-coated cells.

To identify the thermodynamics and the kinetic parameters governing the assembly reaction, the group analyzed the rate of cell- cell contact formation under variety of reaction conditions. They were able to observe the predictable kinetic properties analogous to molecule reacting in solution. They also demonstrated that cell surface DNA density directly affects the assembly. The purification of desired multicellular structures from unwanted byproducts and individual unreacted cells was achieved by synthesizing multicellular structures that consist of red-and-green labeled Jarket cells which can efficiently be sorted out with desired fluorescence properties.

To summarize this study, with a use of a highly versatile cellular bonding agent-duplex DNA, the 3D microtissues were assembled by building connectivity among cells. This process could be done in a typical cell culture conditions and does not require genetic modification as well as the multicellular products are portable to any environment for fundamental studies or tissue engineering.

2.2   3-D Microwell Culture of hESCs

As differentiation and proliferation capabilities of stem cells are widely known it is important to understand that the hESC have unlimited capabilities to indefinitely proliferate and differentiate into each of the three embryonic cell lineages. These hESCs are usually derived from early stage blastocyst human embryo inner cell mass. A great deal of care has to be taken in order to maintain the hESCs undifferentiated in culture, since more often it shows spontaneous differentiations. These spontaneous differentiations are often presumed to be the effect of cell-cell contact, soluble factors or cell-matrix signaling cues. Trivially the hESCs are cultured with mouse embryonic fibroblast (MEF) feeder cells or MEF conditioned medium in ECM[5].

From different studies performed for understanding the differentiation pattern or signaling, it can be clearly conferred that microenvironment has a huge influence on stem cell differentiation. And also the fact that the differentiation of stem cell is initiated and stimulated only after formation of cellular aggregates known as embryoid bodies (EBs). EBs size and shape also have been reported to influence and direct the differentiation. This group has developed a system that controls hESC colony that implies controlling of EB size by combining chemical and physical restraints. The hESC grow beyond 2D layers after confluencing, founding cell aggregates[25]. 2D microcontact printing (μCP) application to hESC are constrained with requirement in z-direction growth. Hence, microwells can be constructed to pattern ECM in order to facilitate the z-directional growth for prolonged culture of cells that are contact inhibited. The approach of culturing the cells in microwells with functionalized ECM adsorption surrounding wells, could prevent the growth of cells outside wells and facilitate only inside wells.

This study described the microwell arrays development that facilitates the hESC culture and EB formation. The well surfaces were functionalized to absorb the ECM proteins that stimulated the proliferation and cell adhesion. Moreover, the defined geometries provided a cultured environment that permits the growth of hESC undifferentiated for several weeks additionally giving control over the recreation of EB size. The group has constructed the two square geometric microwells that spanned 50 and 100μm laterally and two different heights of 50 and 120μm to assess the growth and differentiation in wells. This was taken into consideration because of the issue that culture has to maintain-localization of hESC to the single microwell and preventing spreading over multiple microwells, secondly hESC must be viable, undifferentiated with maintaining pluripotency after extended periods. Lastly these hESC must be able to be passed into standard dish culture conditions.

hESC localization was achieved by covering the outer surface of wells with gold and assembly of self-assembled monolayer (SAM) of EG3-terminated alkanethiols for preventing of protein adsorption, represented in Fig. 2.1. And Matrigel solution was used on the well inner wall that promote cell adhesion where gold layer wasn't covering. This setup resulted in homogenous distribution of identical shape and size of wells that yielded cell localization within a day after cell seeding which needed about a one week to reach confluency[5], shown in Fig. 2.2. The group has successfully demonstrated the viability and undifferentiated growth of hESC with the microwell along with investigating the possibility of passaging these hESC into standard culture conditions. Homogenous EBs were generated from these hESCs cultured microwell aggregates by carefully minimizing the shear during

medium exchange and let the colony grow extended into the medium above well. The hESC aggregates that are expanded above the microwell could be easily taken into medium by pipetting gently, leaving confluent layer within the microwell. To summarize, this study reported the 3D microwell system for longer period culture and homogenous EB formation with negligible effects on viability and pluripotency of undifferentiated hESC.
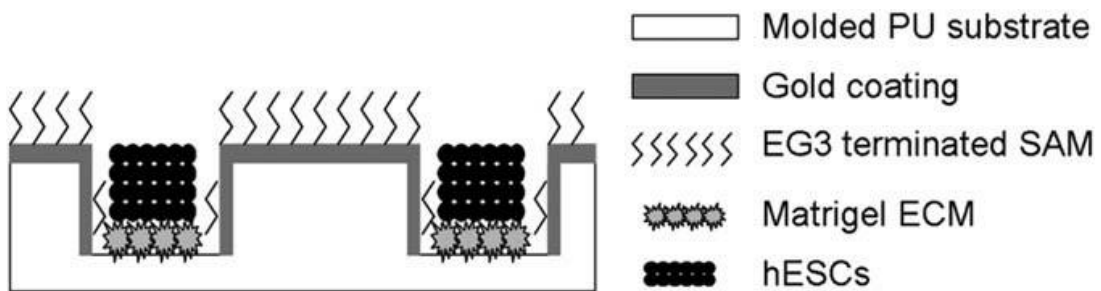

Figure 2.1 Schematic of microwell fabrication depicting localization of physical and chemical constraints to hESC attachment and propagation by Mohr et al.
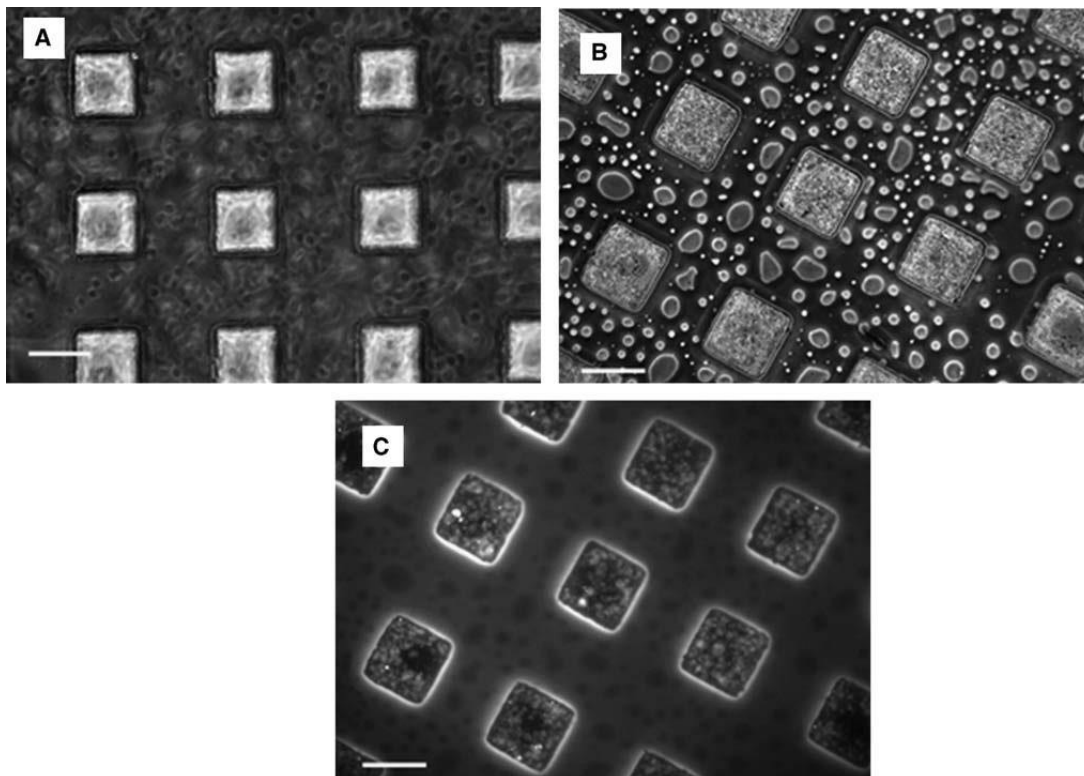

Figure 2.2 Localization of hESCs to microwell. A) microwell prior to cell seeding, B) and C) hESC localization within microwell after 21 days of culture by Mohr et al.

16

2.3   3-D ECM-mediated Neural Stem Cell Differentiation in a Microfluidic Device

Recent advancements in stem cell research has unveiled the development of stem cell based functional therapeutics for diseases like neurodegenerative disorders and central nervous system (CNS) injuries. It has been known for long that 3D microenvironment including ECM and cellular components guides the neural stem cell (NSC) differentiation towards specific lineages through mediation by cell-cell interaction, cell-matrix interaction. This study reported a novel method of quantifying the effects of *in vivo* like ECM for directing the NSC differentiation in 3D microenvironment by quantitative real time polymerase chain reaction (qRT-PCR).

3D microfluidic based assays have been developed to offer more physiological biomimetic culture conditions in *in vitro* models.   These microfluidic devices provides control over spatial and temporal behavior of microscale fluids in contrast with macro scale fluids behavior, allowing replication of *in vivo* like microenvironment. Previous studies on stem cells using microfluidic systems focused primarily on effects of soluble factors on NSC differentiation while other characterize the physical, mechanical, chemical cues for differentiation[26]. Moreover, these microfluidic systems lack the quantitative analysis of microenvironmental effects.

The group presented the novel microfluidic device that made qRT-PCR analysis feasible to quantify NSC differentiation. The device was made of three channels that comprise of one control channel for NSC culture in ECM and to lateral side channels provided a path for supply of growth medium. After culturing and inducing the NSC differentiation the quantification by qRT-PCR was carried out about 4 days later.

2.4   Control of hESC Colony and Aggregate Size Heterogeneity Influences the Differentiation Trajectories

This study is similar to the other studies performed to understand the endogenous parameters influencing the pluripotent ESC differentiation. They pointed out that the differentiation trajectories in EB induced differentiation is influenced by 3 factors including: input hESC composition, EB size and colony size. Several valuable efforts have been made in developing techniques to control the differentiation towards functional cell and tissues. It is assumed that the differentiation in EB recapitulates the embryonic development process. Although the local inductive signaling and microenvironment has been identified to play an

instrumental role in the convergence of specialized tissues into mature functional cell types by differentiation[27].

Bauwen's group has developed the multistage EB based differentiation method taking advantage of μCP technique to control colony and EB size. By generating homogenously sized colonies and EB's the group recognized the need to optimize the maximization of endogenous mesoderm cardiac induced hESC differentiation. Human ESC were maintained on irradiated MEFs in knock-out Dulbecco's modified eagle's medium (ko-MEM). Cell passaging was done every 4 days by dissociating small clumps of cells. Matrigel patterning was carried out by following established protocols of μCP. 2-3 days confluent micropatterned hESCs were pipetted out of the dishes and resuspended carefully, to preserve colonies in hESCs differentiation medium to form EBs. The cells in hESCs colonies and suspended aggregates were quantified using fluorescent-DNA binding dye staining of cells. Aggregates were transformed into suspension of ultra- low attachment non-tissue culture treated plates for 4 days to induce differentiation of EB in cardiac growth.

This study demonstrated the generation of control size EBs using micropatterning hESCs colonies at defined diameter. EB size influence the differentiation fate since this parameter may modulate the spatial signaling with aggregates. The influence of colony size was investigated and quantified using simultaneous analysis of hESCs colonies patterned at 3 different diameters and with non-patterned colonies, on the differentiation trajectories. Gene expression was analyzed after qRT-PCR and compared between the input hESCs population and 2 to 3 days colony size-controlled MP-hESC derivatives.

Non-MP and 200μm diameter MP colonies maintained gene expression levels as their inputs, whereas 400μm MP and 800μm MP has shown drastically increased level of gene expression, reflecting the influence of EB size on differentiation[27]. Narrower size distribution of EBs was observed in MP-EB cultures in contrast with non-MP-EB. Similarly different size EBs were observed with hESC colonies of different diameters and as mentioned previously.

Thus, to summarize, this study reveals that EB based differentiation is a powerful system that mimics the embryonic development process *in vivo* and also provides essential platform to study cell to cell interaction and spatial organization for specific cell type growth. Alongside this also explores the effect of size of hESC-EB on its differentiation fate.

2.5 A Microfluidic Trap System Supporting Prolonged Culture of hESCs Aggregates

Tight regulation of the microenvironments are reported to manipulate the unlimited proliferation and differentiation capacities of hESCs. Intracellular interaction, cell- matrix signaling and soluble factors are a few things in the pool of differentiation influencing factors. This particular study demonstrated the prolonged culture of EBs that are essential for inducing stem cell differentiatio on a microfluidic system that enables the culturing of the cells, closely mimicking the biological microenvironments.

Huge variations in cell lineage profiles are found between EBs grown within the same culture. This reflects the importance of microenvironment regulation. Different studies explored that the differentiation is directly affected by EBs size, since a minimum number of cells were needed to form the cell aggregates designed to induce hematopoietic cell differentiation[4]. At the same time, Mohr et al. 2006 has reported and demonstrated the relationship between EBs shape and differentiation fate in extended pluripotency and self-renewal of EBs growth in unconstrained EBs to microwell grown EBs. Additionally, hypoxic conditions are often observed in developing embryos suggesting the fact that oxygen tension in the microenvironment alters the differentiation of EBs. For example, the concentration of oxygen influenced the cardiovascular morphogenesis, bone morphogenesis, mammalian placentation and stem cell fate[28]. Hence, it is presumed that the geometry and microenvironment in atmosphere of EBs if manipulated accordingly, give a great deal of direct control over their differentiation fate helping in correlating with *in vivo* embryonic differentiation.

Recent advancements in the microfabrication technology allow fine-tuned culture managements by means of control and reproducibility of extracellular cues to the levels that are highly unachievable by standard tissue culture. This study demonstrates a microbioreactor that has been tailored to enable prolong EB culturing which includes thousands of microtraps for single ESC trapping and positioning for aggregation, prolonged culturing by effective exchange of gases and nutrients that provided optimize conditions for sensitive EBs. Finite element simulations were performed to understand the flow and exchange of gases and nutrients to optimize the design that was crucial in maintaining the size of EBs to a particular level by using continuous flow avoiding the growth of EBs outside the trap opening. Special trap geometry also helped consistent gas and nutrient exchange and maintained a uniform number of cells for aggregate formation[29].

The device was fabricated using standard lithographic procedures, comprised of 8 interconnected channels having same flow resistance in the fluidic network shown below in Fig. 2.3. This allows a more homogenous distribution of cells while seeding. The entry-point of each channel was specially equipped with the cylindrical cavity to capture small bubbles. An appropriate mass transport model was constructed to ensure normal cell growth since the high surface to volume ratio proves to be limiting factor for oxygen and nutrient levels. The model was based on mass continuity equation for diluted species and steady state Navier-Stokes' equation for Newtonian flow. Convection-Diffusion equations are solved by

$$\rho_f(\frac{\partial \overline{u}}{\partial t} + \overline{u} \cdot \nabla \overline{u}) = -\nabla P + \mu \nabla^2 \overline{u} \tag{2.1}$$

$$\nabla(-D\nabla c) = R - u.\nabla c \tag{2.2}$$

D – Isotropic diffusion coefficient of oxygen in water, c – concentration, u – velocity field, R – oxygen consumption rate (OCR) of cells, P – pressure, ρ_f – fluid density and μ - fluid viscosity. OCR was set according to the Michaelis-Mentin kinetics with respect to oxygen for bulk of EBs as

$$OCR = V_{max} \frac{C}{C + K_m} \tag{2.3}$$

C – Oxygen concentration, V_{max} – maximum consumption rate and K_m – Michalis-Mentin's constant. OCR is constant at higher oxygen ($C >> K_m$) to V_{max} which reaches zero at low oxygen ($C << K_m$).
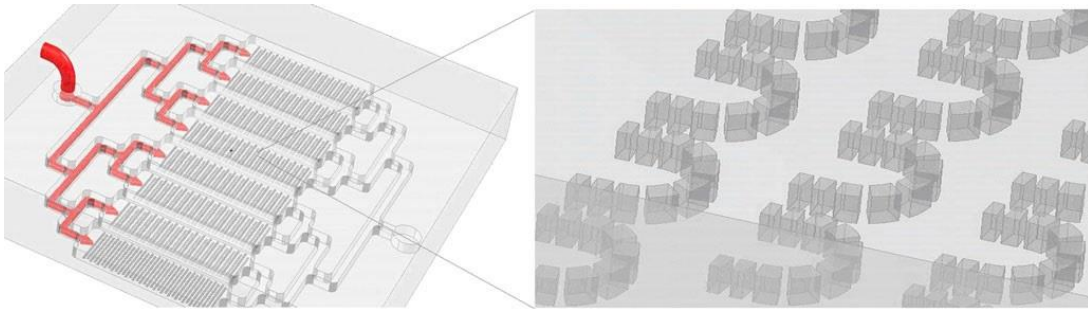

Figure 2.3 Illustration of the microfluidic device: micro-bioreactor setup by Khoury et al.

Different trap sizes were used to evaluate the constraints put on differentiation due to EBs size. The viability of the cells were determined resulting that vast majority of EBs

were made up of live cells. Tools to generate temporarily and spatially synchronized EBs are crucial in order to recapitulate developmental process of early hESCs. The earlier reports control initial size and shape of EBs but fail to maintain culture for longer periods. Hence this system of microfluidic traps proves to be important milestone for maintain and prolonged culturing of hESCs differentiation over long periods along with sustaining viability. Additionally, the automated techniques for microscopic imaging and image processing can be applied to monitor each aggregate due to the advantage of aggregate positioning at a defined position or location.

2.6   Cell Patterning Chip for Controlling the Stem Cell Microenvironment

Diffusible signaling and cell-cell contact are parts of cell-cell interactions that is a vital parameter in numerous biological processes like tumor growth, atherosclerotic plaque formation[30], and also in stem cell differentiation. These have been proven to be vital in tissue engineering and organ replacement therapies. These signaling can be modulated *in vitro* in several ways, but these approaches are limited to known molecules or single molecular manipulation. Alternate approach is modulation of cell positions while seeding. This traditional cell culture limits the position modulation at macroscopic level that can be varied only by varying cells seeding density. Thus, precise control of cellular microenvironment that involves manipulation of cells position at singe cell level is called cell patterning.

This study shows the developed Bio Flip Chip (BFC) for patterning of cell apart from the different existing techniques such as μCP, switchable substrates, elastomeric stem cells, microwells[31], optical tweezers, electrophoresis and DEP etc. All the existing technologies are very useful for their developed applications, however, are limited in single cell patterning with varying substrates and proliferation monitoring over time. These may impose the requirement or restriction on selecting the substrate such as requiring specific surface chemistry, electrodes, optical transparency etc. The BFC is seen to be free from these limitations and provide a simple means to pattern single cells.

The developed BFCs consist of thousands of microwells fabricated using a polymer, each sized to trap down single cells. Cells are pipetted on to surface of the chip allowing it to fall into the well. After trapping, the microwells and other cells are rinsed away and then the BFC is flipped up-side down on the desired substrate. The cells then fall out of the microwell onto substrate and gets attached after few hours[32]. Figure 2.4 describes the device and operation.
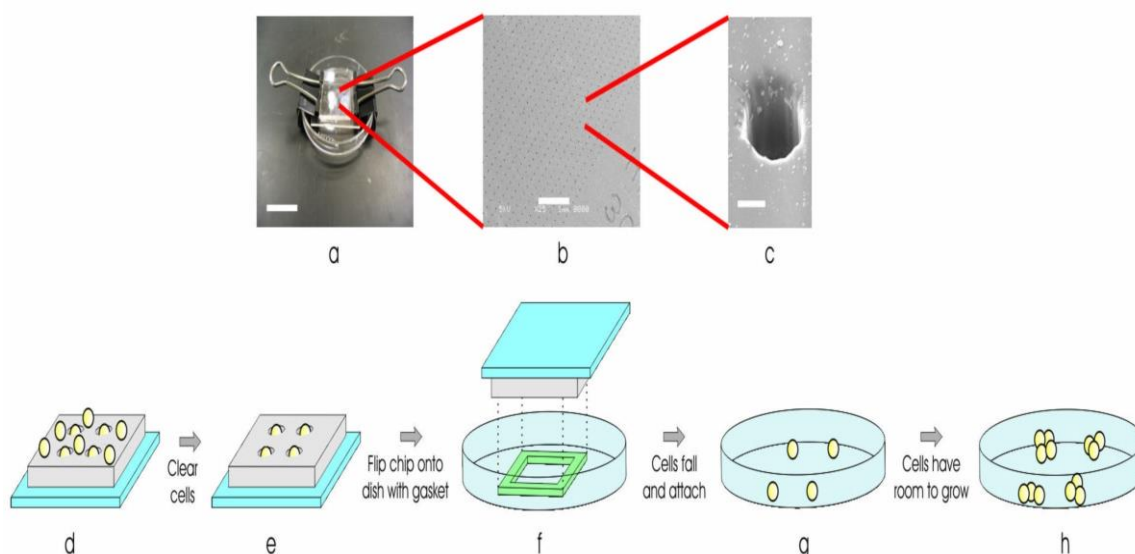
21

Figure 2.4 BFC device and operation a) BFC packaging, b) SEM of microwells, c) SEM image of single microwell, d) cells pipetted onto surface, e) cells trapped in microwell, f) BFC flipped upside down in culture dish, g) cells fall out of microwells onto the surface and attaches after few hour and h) cells have room to grow and move, studied by Rosenthal et al.

This approach to precisely control the cell patterning with single cell resolution has numerous advantages: There is no requirement of any external equipment of chemicals to pattern that make it easily adaptable for any lab. In this paper, the authors have explained the fabrication and operation of the BFC which is outside the scope of this thesis. This technology can offer the combination of different capabilities including patterning of cells with single cell resolution, large number of cell patterning, allowing patterns to grow and move, variations in substrate of patterning, being gentle on cells and easy to use[32].

2.7 Magnetic Manipulation and Spatial Patterning of Multi-cellular Stem Cell Aggregates

Tissue engineering is capable of serving and constructing the models of healthy and disease tissues for diagnostic, drug screening platforms and also for organ replacement or regenerative therapies[33]. This seeks the mimicking complexities of native tissues and organs. Directed assembling of heterogeneous and homogenous population of cells is needed for 3D multicellular neo-tissues.

Existing protocols and approaches for such 3D multicellular assembly control and patterning are dependent on the modification of cellular interactions and intrinsic adhesive properties of cells. Usually intercellular adhesion is extenuated by natural cell-cell adhesion

or by chemical surface modification of cells to enhance and stabilize the multicellular assembly. But, an extremely concerning point in this approach is the probability of attenuating or inhibiting the signaling pathways of stem cells that are explored to influence the differentiation. Other defined approach is entrapment of cells within the biomaterial like hydrogel which then can be assembled by chemical and physical properties alteration of cells. However, the properties of hydrogel like stiffness, degradability can independently or mutually contribute to alter the phenotype[34], and hence need a cell specific design criteria. Both the above approaches need a priori design of parameters for cell adhesion mechanism, design material that are function of cell type and construct geometry.

Khoury et al. demonstrated in this study a robust approach that is capable of multi-scale assembling of variety of cells without any surface and chemical modifications using magnetic forces. Magnetic forces have long been used for large scale applications including sorting, separation of cell population, due to the broadly spread forces that span over long range of length scales[35]. In general, these approaches to direct cells by magnetic labeling requires the surface properties of magnetic particles and/or the cells for greater association. Alternative is inducing magnetic sensitivity in cells by Endocytosis, however these can interfere with the intra cellular signaling and viability[6].

The group has presented the efficient and stable incorporation magMPs in the dose dependent manner in extracellular environment of 3D aggregates of stem cells that does not incur any surface adhesive properties modifications or biochemical modifications of cells. These magMPs incorporation enables the directed movement and assembly of spheroids by applying external magnetic field which can yield a complex 3D constructs across broad length and timescales[6]. EBs were formed using single cell suspension by forced aggregation in microwell inserts. The magMPs that are made up of polystyrene microparticles of 4μm diameter were added at 1:10, 1:3, 1:1, 3:1 MP to ESC ratio. The pelleting of magMP was performed using a centrifugation or a magnetic pull down by a magnet placed below plate. These aggregates were transferred to a suspension culture on a rotary orbital shaker that maintains population of spheroids to be homogenous.

Magnetic manipulation was achieved using 4 x 1 mm Nickel-plated Neodymium magnets to spatially confine the spheroids location in suspension culture. Different patterns of spheroids can be formed by configuring the magnets in desired shape and placing it opposite to suspension culture dish. The efficiency of pattern is dependent on distance of the magnets from the magMP, i.e. the culture medium. Incorporation of magMPs was achieved using sequentially seeding mESCs and magMPs to the microwells and then centrifugation and magnetic pull down. The EBs formed by incorporation of 1:10 and 1:3 magMP to ESC

ratio were sufficiently sensitive to magnetic force. Hence, further analysis was done using these EBs. The addition of magMPs showed no effect on morphology, neither altered the cellular organization. The viability of hESCs was observed between EBs with and without magMPs incorporation which resulted in a negligible effect on cell viability.

The ability of the device to manipulate the spatial positioning and truncation of stem cells was examined in both static and dynamic culture systems using external magnetic field. Entire fields of spheroids could be concentrated, displaced and rotated base on the relative location, direction and manner in which the field is applied under static culture condition. Higher density magMP spheroids dominantly showed more sensitivity to the field compared to the one with low density of magMPs. The magnetic control in dynamic culture condition was investigated by use of patterned magnetic field to constraint the spheroid location within orbital shakeup that is assumed to be used to maintain the homogenous population of EBs in suspension culture conditions. Generally, due to rotary motion, the spheroids occupy a focused region of the dish that changes slightly on each rotation. The location of spheroids were confined to the region below the magnetic pattern and observed with different patterns. Thus, incorporation of magMPs in extracellular space of stem cell spheroids provide a fluent mains to control the spatial patterning of EBs in dynamic and static culture conditions. This can be easily implemented and can help in addressing the significant unanswered questions in the field of stem cell biology, tissue engineering and cell bioprocessing.

The above chapter has mainly discussed different studies carried out for stem cell differentiation, the effects of size and shape of EB formed on differentiation fate and trajectories. It has also explored the ways of controlling and manipulating the cells, concentrating the cells to form spheroids and directed special patterning of cells, to recapitulate the embryonic development process ex vivo. However, each study has its limitations and setbacks like providing culture efficiently but have no control over patterning. Some provided the ability to pattern spheroids by utilizing standard cultured conditions in dish. Also there are almost negligible studies which uses advanced microfabrication technologies to its full potential.

Here, we report a novel microfluidic design to develop a device that allows spatial patterning, manipulation and aggregation of stem cell by micropatterning magnets on chip. To analyze the effects of magnetic field on magMP incorporated stem cells, a numerical priori design is constructed to evaluate the optimal parameters for obtaining the desired results. Following chapters presents the modeling of the device and numerical simulations.

Chapter 3

Device Modelling

In microfluidic devices, especially in cell perfusion and cell cultured devices the oxygen, nutrient levels and medium composition present limiting factors due to high surface area to volume ratio. Hence, it is important for an engineer to construct a model that ensures the cell survival and normal growth with the help of appropriate mass transport model. This model is based on Navier-Stokes' equations for a Newtonian fluid, magnetic force equations and convection-diffusion equations.

3.1   Magnetization Governing Equations

Magnetic permeability of a material (µ) quantifies the ability of magnetic field lines to reach a certain density within a material whereas the number of field lines per unit area is coined as magnetic flux density B (SI unit Tesla). It has been demonstrated and postulated that the field density decreases rapidly with increasing distance from the magnetic surface. However, the distance is in millimeters where the field dies off, which is much larger than electrical fields ranging in nanometers, hence allowing efficient application in microfluidics. Magnetic field is present in the surrounding area of permanent magnets or a wire carrying current in which a force is experienced.

According to the magnetic susceptibility (χ), materials are classified into: diamagnetic, paramagnetic, and ferromagnetic materials. Diamagnetic materials ($\chi < 0$) are repelled from magnet, i.e. they are moved towards magnetic minima in the field. Paramagnetic magnetic materials ($\chi > 0$) experience a small force towards the magnetic field maxima and hence are attracted towards magnet. Ferromagnetic materials ($\chi \gg 0$) such as Ni, Co, Fe are strongly are attracted towards magnetic field.

In order for cells or particles to be able to concentrate, it is important to understand the force and field distributions in the channel. The magnetic force is given by equation (1.6):

$$F_m = \frac{V(\Delta\chi)}{\mu_0}(\overline{B}\cdot\nabla)\overline{B}$$

Where volume of the particle $V = \dfrac{4}{3}\pi a^3$ for a spherical particle of radius a, B represents magnetic flux density in Tesla, μ_0- permeability of free space $\mu_0 = 4\pi \times 10^{-7}$ NA^{-2} and $\nabla = \left[\dfrac{\partial}{\partial x}, \dfrac{\partial}{\partial y}, \dfrac{\partial}{\partial z}\right]$ is a gradient operator.

Since we need aggregation of the cells, we are ought to deal with z-component of force F_m given by F_{mz} as:

$$F_{mz} = V\frac{(\chi_p - \chi_m)}{\mu_0}(B_x \frac{\partial B_z}{\partial x} + B_y \frac{\partial B_z}{\partial y} + B_z \frac{\partial B_z}{\partial z}) \tag{3.1}$$

The field distribution of flux density B is calculated using magnetic field no current interface from AC/DC module of COMSOL. The governing equations and mathematics involved are explained below.

Problems of electromagnetic analysis deals with the solving Maxwell's equations that are subjected to specific boundary conditions. Different forms of Maxwell's equations states the relationship between fundamental quantities.

E-electric field intensity

D-electric flux density

H-Magnetic field intensity

B-Magnetic flux density

J-current density and

P- Electric charge density, equations are written as:

$$\nabla \times H = J + \frac{\partial D}{\partial t} \tag{3.2}$$

$$\nabla \times E = -\frac{\partial B}{\partial t} \tag{3.3}$$

$$\nabla \cdot D = \rho \tag{3.4}$$

$$\nabla \cdot B = 0 \tag{3.5}$$

The first two equations are also referred to as *Maxwell-Ampère's law* and *Faraday's law*, respectively. Equation (3.4) and (3.5) are two forms of *Gauss' law*: the electric and

magnetic form, respectively. The constitutive relationship describing the properties of medium are-

$$D = \varepsilon_0 E + P$$

$$B = \mu_0 (H + M) \tag{3.6}$$

$$J = \sigma E$$

Where, ε_0 - permittivity of vacuum, μ_0 -permeability of vacuum and σ- electrical conductivity. P represents electrical polarisation vector. M vector describes how the material is magnetised, when a magnetic field H is present. Permanent magnets have a non-zero M even when no magnetic field is applied in its surrounding. Linear materials have relationship:

$$M = \chi_m H$$

Therefore, $B = \mu_0 (1 + \chi_m) H = \mu_0 \mu_r H = \mu H \tag{3.7}$

In this equation μ_r is relative permeability of medium.

General form of the material constitutive relationship is given by:

$$M = \mu_0 \mu_r H + B_r \tag{3.8}$$

For non-linear materials, B_r-is remanent magnetic flux density which is the magnetic flux density when no field is present.

Since, the demand of the problem is having no current, we have used the magnetic field no current interface. This study is a stationary study that also supports time dependant study having no changes in the equations. The interface solves Gauss' law of magnetic flux from above equations using scalar magnetic potential (V_m). The dependant variable V_m can be solved from the relationship $H = -\nabla V_m$

This is a current free medium where, $\nabla \times \mathrm{H} = 0$, that explains that V_m can be defined from above equation, hence,

$$\nabla \cdot B = 0 \qquad \text{becomes} \qquad \nabla \cdot (\mu_0 (H + M)) = 0$$

$$\Rightarrow -\nabla (\mu_0 \nabla \mathrm{V}_m - \mu_0 \mathrm{M}) = 0$$

The default force calculation involves Laurentz Force given by $F = J \times B$, but here we define our own equation using the flexibility of COMSOL given by equation (3.1).

3.2 Laminar flow and Governing Equation

The fluid in the channel can be modelled using laminar flow interface, this single fluid flow interface is based on Navier-Stokes' equations that read as

$$\frac{\partial \rho}{\partial t} + \nabla \cdot (\rho \bar{u}) = 0 \tag{3.9}$$

$$\rho \frac{\partial \bar{u}}{\partial t} + \rho(\bar{u} \cdot \nabla)\bar{u} = \nabla \cdot \left[-P\bar{\bar{I}} + \bar{\bar{\tau}} \right] + F \tag{3.10}$$

τ- Viscous stress tensor, F- volume force vector (N/m^3).

Equation (3.8) represents conservation of mass with continuity equation whereas, equation (3.9) is a vector equation representing conservation of momentum.

Above equations are modified according to compressibility of fluid, in this study fluid is assumed to incompressible, since temperature variations are negligible i.e. ρ is constant.

$\tau = \mu \nabla u$, and hence equation (3.8) and (3.9) become

$$\rho \nabla \cdot u = 0 \qquad \text{and}$$

$$\rho \frac{\partial \bar{u}}{\partial t} + \rho(\bar{u} \cdot \nabla)\bar{u} = -\nabla P + \mu \nabla^2 \bar{u} + F \tag{3.11}$$

(Transient term)   (Convective term)   (Inertia term)   (External force)

Reynolds number is fundamental quantity in analysis of fluid flow given by:

$$R_e = \frac{\rho U L}{\mu} \tag{3.12}$$

U- velocity scale, L- representative length.

Reynolds number is the ratio of inertial forces to viscous forces.

At low R_e number, viscous forces dominate inertial forces and hence damp out all the disturbances, which leads to a laminar flow. At high R_e number, damping is reduced that gives rise to small disturbances to grow by non-linear interactions. And at very high R_e the fluid flow ends up being in a chaotic state called turbulence.

It is automatically calculated in the interface as

$$R_e^c = \rho |u| h / (2\mu)$$

$$\Rightarrow h = L, |u| \text{ is for } U$$

To solve the partial differential equations (PDE), boundary conditions are necessary. Here as the flow is laminar, we can incorporate no slip boundary condition at all the walls except inlet and outlet, as $u = 0$ at side walls and top-bottom surfaces of channel. Inlet and outlet boundary conditions implies in the large variety of Navier–Stokes' equations behavior ranging from completely elliptic to completely hyperbolic.

Inlet requires specification of velocity fluid which is the most robust way. Another way of prescribing this is using pressure specifications that indirectly specifies normal velocity component from continuity equation as:

$$-P + \mu \frac{\partial u_n}{\partial n} = F_n \quad , \quad \frac{\partial u_n}{\partial n} \text{ is the normal derivative of normal component of}$$

velocity field.

Similarly, at outlet, the common method is the prescription of pressure condition at outlet. Often this is not sufficient, hence an alternate approach is supplementing it with a condition on tangential velocity component given by.

$$\mu \frac{\partial u_t}{\partial n} = 0 , \qquad \frac{\partial u_t}{\partial n} \text{ is the normal derivative of tangential velocity component.}$$

3.3 Governing Equations for Concentration

To understand the transport and tracking of cell behavior a mass-continuity equation that is convection diffusion equation is needed. This is derived from Fick's Law ($j_D \propto c$) where c represents concentration in particles per unit volume, j_D represents diffusive flux

$$j_D = -D\nabla c \quad \text{, where } D \text{ is diffusion coefficient in m}^2/\text{s}$$

Similarly, convective flux is given by:

$$j_C = uc \quad \text{thus, convection diffusion equation is reduced to}$$

$$\frac{\partial c}{\partial t} + \nabla \cdot j = R$$

$$\therefore \quad \frac{\partial c}{\partial t} + \nabla \cdot (-D\nabla c + uc) = R$$

$$\therefore \quad \frac{\partial c}{\partial t} + \nabla \cdot (-D\nabla c) = R - u\nabla c \tag{3.13}$$

Here we want to identify the aggregation due to force field applied using magnet. Hence equation is modified accordingly to constitute the effect due to magnetic force. Required particle concentration field can be given due to the joint effect of magnetic forces, particle Brownian motion and convective flux by adopting from Pham[36]

$$\frac{\partial c}{\partial t} + \nabla \cdot [-D\nabla c + c(\gamma F_{mz})] + \bar{u} \cdot \nabla c = 0 \tag{3.14}$$

(Transient term)   (Diffusion term)   (Magnetic term)   (Convective flux)

Where, $D = \mu k_B T$, μ- represents particle mobility given by

$$\mu = \gamma = \frac{1}{6\pi\mu_b a} , \quad \text{where } \mu_b \text{ defines dynamic viscosity of the liquid.}$$

$k_{B\text{-}}$ is Boltzmann constant $k_B = 1.3806 \times 10^{-23}$ JK^{-1}.

The necessary boundary condition associated with the equation are Dirichlet condition where particle concentration is known '$c = c_0$' or the convective flux Neuman boundary condition at walls ($\nabla c \cdot \mathbf{n} = 0$) that is normal derivative of concentration is zero. At the outlet respective condition is due to convective flux.

In our model we used normalized concentration as $c^* = c/c_0$ -a dimensionless quantity in place of c throughout the PDE interface.

3.4   Model Geometry

To start the modelling and understanding the distributions of flux density force field and velocity fields it is crucial to optimize the geometry of the device. We started with a simple 3-D model that constitute a glass layer at bottom, a single rectangular magnet patterned on the substrate , a polydimethylsiloxane (PDMS) mold to cover the magnets which is not bio compatible, and the channel above this PDMS lid is covered with another PDMS having channel fabricated.

Typical microfluidic devices vary in their sizes in mm as a whole device. Here we modelled the device with dimensions 4.5 X 2.5 X 0.75mm. Two different patterns were modelled with two different directions of magnetization. The first model is shown in Fig. 3.1, which consist of single magnet of size 200 X 200 X 100µm. The rationale behind selecting this particular dimensions was the EBs formed due to aggregation were typical of the diameter of 200µm and was adapted from the Khoury et al.[29] study and Farrokh et

al.[37]. Other geometries in Fig. 3.1, show a 2 X 2 and 4 X 3 magnetic array patterned on the substrate that can utilize the full potential and space in the device.
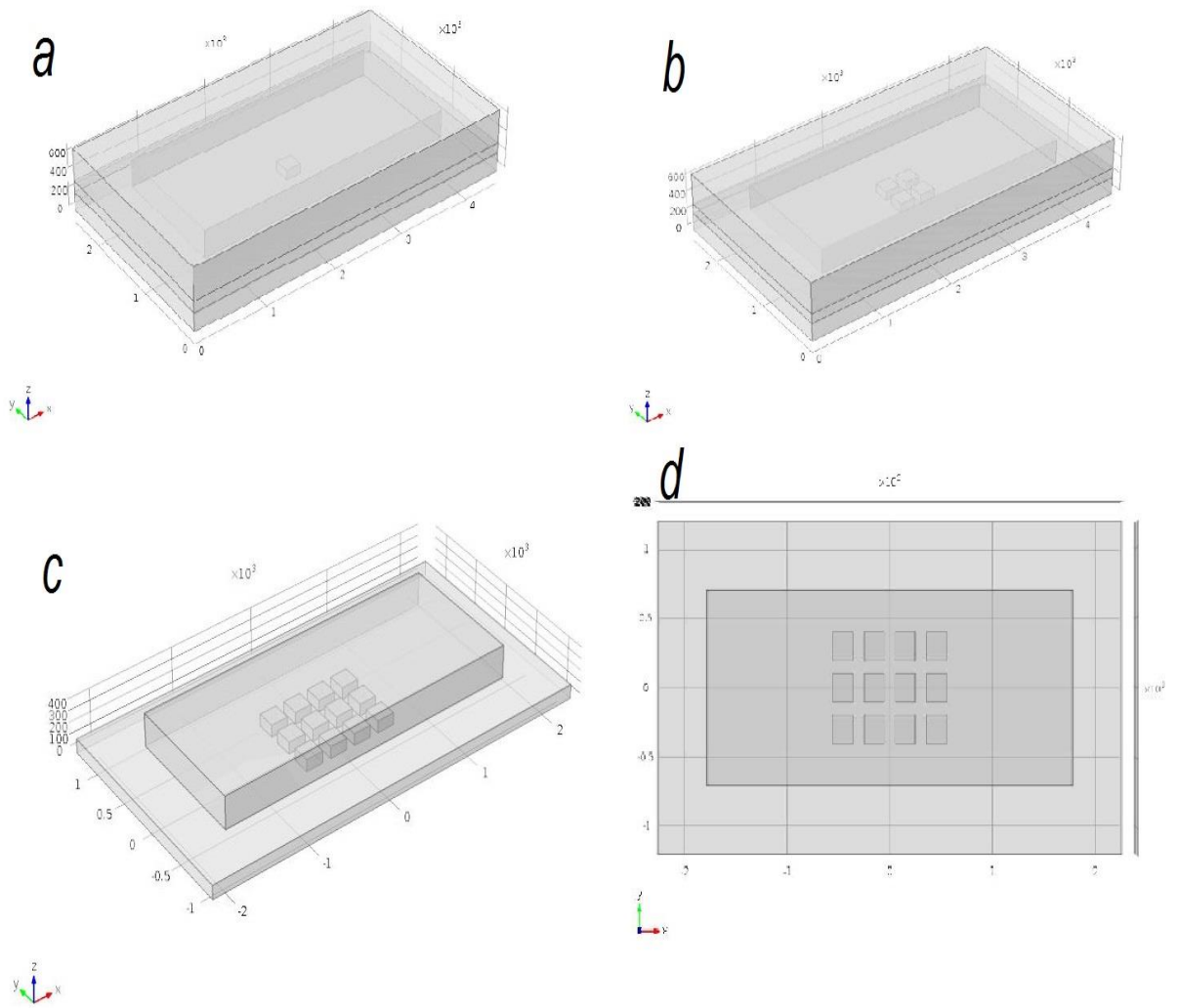

Figure 3.1 Shows different geometries used in the study a) single magnet at center b) 2 X 2 magnetic array and c) 4 X 3 magnetic patterned each 100µm apart, and d) top view.

3.5 Materials and Parameters

Different materials that are assumed to be involved in device fabrication are incorporated in the model by specifying parameters needed for different physics interfaces. The substrate used was glass substrate on which thick NdFeB magnet would be patterned using standard fabrication procedure which will involve high speed triode etching for magnetic patterns. Magnet and the channel interface was isolated with PDMS layer so as to avoid direct contact of cells with magnets which is not bio compatible. The fluid channel was in grooved in the PDMS mold.

The properties of the materials in the model are listed in Table 5.1 Basic properties of materials used in simulations, which include magnetic susceptibility (adopted from work by Farrokh et al.[37], relative permeability, viscosity and density etc.

3.6 Solver Configuration

Initial studies were progressed by using advantage of performing different studies of each physics interface separately in a single model that can be combined at any stage to avoid memory constraints of computation.

Magnetic field no current interface and laminar flow interfaces studies were carried out using direct coupling method in segregate solver configuration. In this configuration MUPMS solver is used. Our user-defined equations were modelled using PDE mathematic interface for studying concentration distribution inside channel. This physics was solved using both MUMPS and Dense Matrix configuration in segregated solver.

The method of termination of solvers were set to tolerance factor and number of iterations, in this case, tolerance factor used was ranging from 0.0001 to 0.000001 while the number of iterations were modified between 60 and 1000 to achieve convergence.

3.7 Meshing

Meshing of the designed modelled constitutes important aspect of numerical studies. We studied 3D geometry of the device hence, most of the domains were meshed using tetrahedral elements while triangular meshing was applied on few edges and boundaries. Convergence of the solution is dependent on meshing elements as well. Similarly, obvious differences can be pointed out in smoothness and fineness of the distributions when comparing extremely finer, finer meshing with normal or fine meshing elements.

Meshing for a single magnet geometry was applied using user-controlled meshing in which, meshing on magnet was applied such a way that maximum element size was 5um, on the other hand remaining geometry was meshed using finer meshing method. Single magnet geometry consisted about 544053 domain, 15060 boundary and 400 edge elements. Total geometry had 687031 domain, 22746 boundary and 826 edge elements after meshing. The second geometry was 4 X 3 array of magnets patterned over the glass substrates. For this particular geometry, in order to simplify the computation, we have removed the glass layer from bottom of the magnets and also PDMS outer cover that will not be having any significance effect on the solutions and fields. This time fully user-controlled meshing was carried out because sudden variations in the field will be observed near the walls of the magnet which lead to dense meshing near the edges and boundaries of the magnets. All domains were extremely fine meshed while few had to be meshed even more than that. The interface of solid and fluid branches at channel base above mesh was meshed separately.

The boundaries of channel excluding top surface and side walls were triangularly meshed using fluid dynamics physics' finer meshing, which has 3.92μm and 36.3μm as minimum and maximum element size. This mesh consisted 20996 boundary and 762 edge elements and is shown in Fig. 3.2a). Remaining boundaries of the major geometry excluding magnets were meshed using general physics finer-sized triangular elements, varying element size from 18μm to 248μm minimum and maximum respectively. This consisted total 26260 boundary while 1084 edge elements. Remaining boundaries of magnets were extremely fine meshed taking fluid dynamics so that maximum element size was 12.7μm whereas minimum as reduced to 0.196μm. This meshing of magnets generated 28652 boundary and 1866 edge elements, shown in Fig. 3.2b).

Remaining domains produced 462721 domain, 38192 boundary and 2044 edge elements when fine tetrahedral meshing was applied which considers 9.8μm and 51.9μm as minimum and maximum element sizes respectively, depicted in Fig. 3.2c). In this way total meshing applied consisted 818590 domain elements, 51542 boundary elements and 2524 edge elements in the pool.
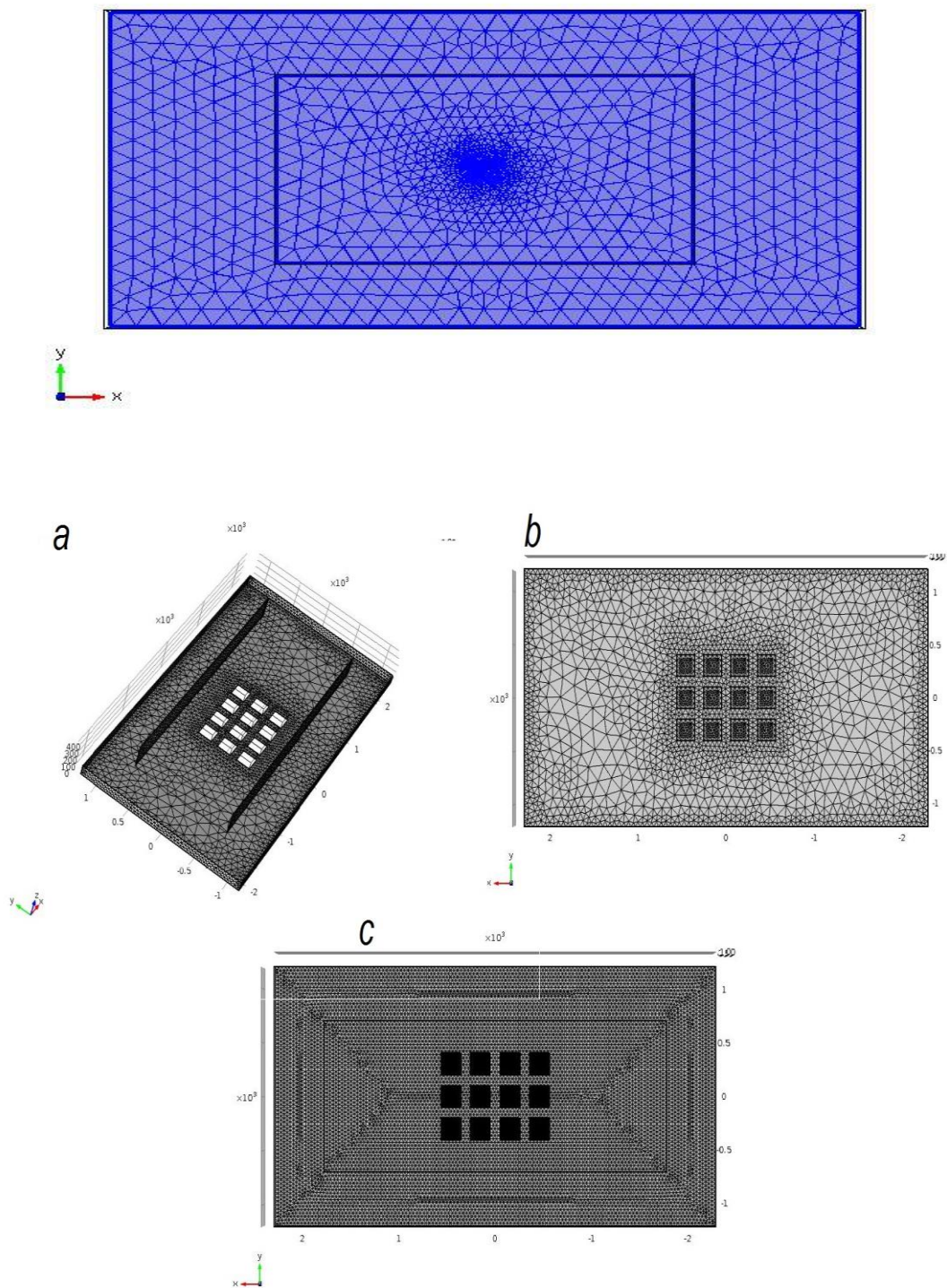
Figure 3.2 Meshing applied: on the single magnet shown at top, and a 4 X 3 patterned geometry. Mesh on: a) inlet, outlet and fluid-solid interfaces boundaries, b) finer meshing near magnet edges and c) extremely fine meshing on magnets.

34

Chapter 4

Results and Discussions

To start with the idea of aggregation of cells using magnetic field generated by micromagnets patterned on the glass substrate, we studied field distributions. First, we used single micromagnet of dimensions 200 x 200 x 100µm. Magnetic flux density generated was plotted at different heights above magnets. The distribution was plotted at 20, 40, 80 and 200µm above magnet in channels shown in Fig. 4.1. This flux density is observed to be maximum at the center above magnet and slightly reduces towards lateral ends since the magnetization was in z-direction. As we gradually increased the height in the x-y plane, we noticed that the field area of maximum flux density reduced to a narrower region and it starts to appear that the flux density pattern as concentric circular field at heights close to the channel height of 250µm, visible in Fig. 4.1c). The magnetic flux density was measured to be maximum in the close proximity of magnets, recording a value of 270mT that is commendable to achieve since, maximum magnetic field that could be generated using 4mm X 1mm permanent magnet is reported to be 400mT[19].

When the same magnet was magnetized in x-direction, field is concentrated at edges of magnet in +x-direction. This concentrated field spreads across the area near to the edge as the distance from magnet is increased in the channel, while magnitude reduces rapidly from 180mT to 60mT at 80µm above magnet, plotted in Fig. 4.2. Since the flux density due to magnetization in x-direction is concentrated mainly at edges of the magnet and the field intensity is also less, we decided to continue with the magnetization in z-direction providing a larger area for concentration to make aggregation possible.

Magnetic flux density was also studied in 2 X 2 and 4 X 3 micropatterned magnets 20µm and 100µm apart. With 2 X 2 pattern, flux density achieved was observed to be similar to the single magnet pattern varying slightly in magnitude ranging 230mT to 10mT at far end in the channel.
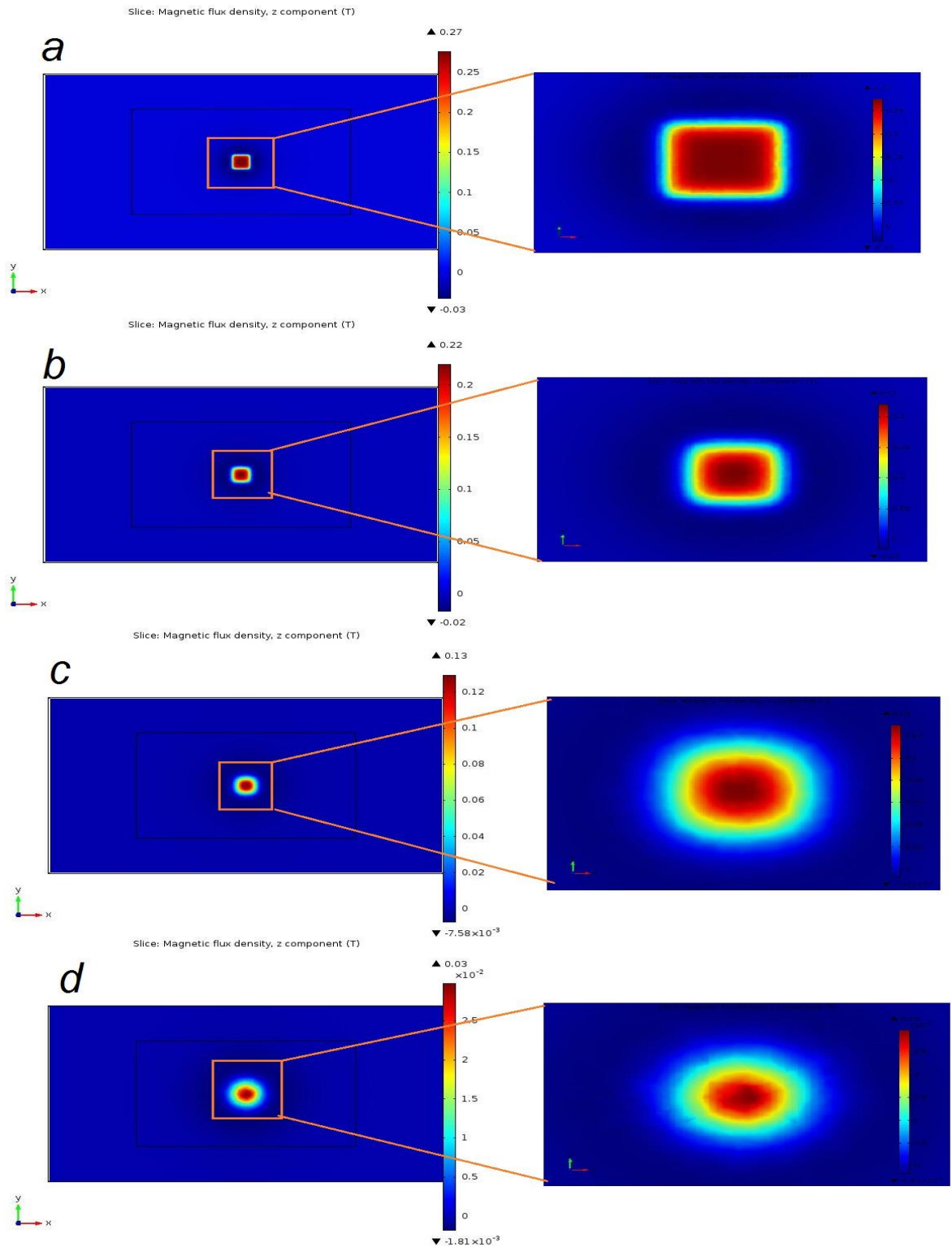
Figure 4.1 z-component of Magnetic flux density (B$_z$) in XY planes, plotted at a) 20, b) 40, c)80 and d) 200μm above magnet in single magnet pattern with Z-directional magnetization, reads maximum of 270, 220, 130 and 30mT respectively. All images on the right hand side shows respective zoom in on the field in Tesla.
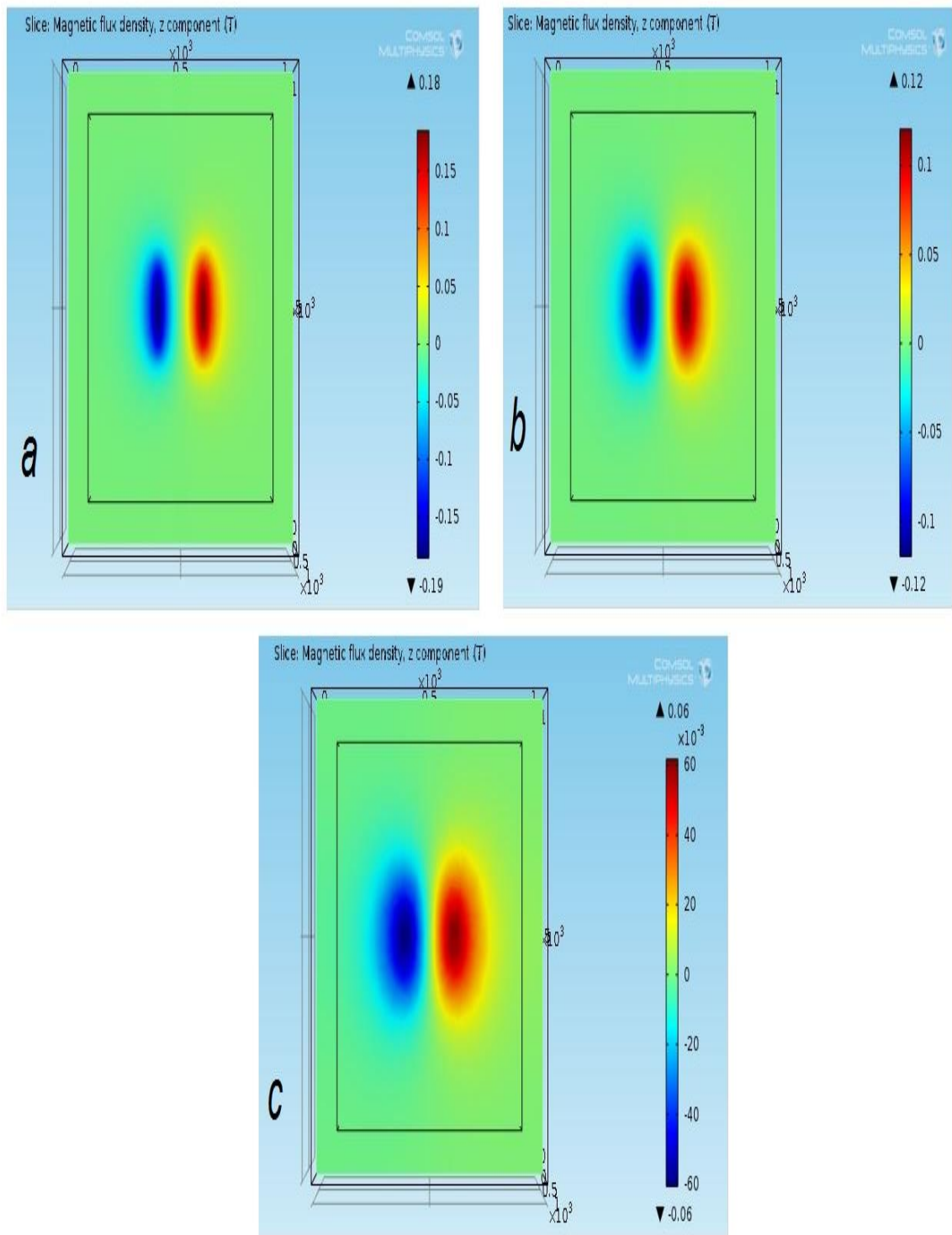
Figure 4.2 Magnetic flux density, z-component (B$_z$) in Tesla, plotted in XY plane due to single magnet with magnetization in X-direction, at a) 20, b) 40 and c) 80μm above magnet in the channel. B$_z$ ranges between (-0.19 to 0.18T) at 20μm and (-0.06 to 0.06T) at 200μm height.

With 4 X 3 magnet pattern, each 20μm apart, the field lines interact with each other to give higher fields at the center above each magnet while minima can be observed at the intersection of the magnetic fields in the empty space between magnets. Increased flux density was found to be 190mT at a height of 20μm above magnet. As the plane of observation moves higher in z-direction, the magnitude reduces, giving a combined effect due to all magnets to maximize the field at the center of whole pattern showing maximum field at the magnet in the middle row as shown in the Fig. 4.3d). Also, the distribution of the field when magnets are patterned each 100μm apart, can be seen in Fig. 4.4 and Fig. 4.5 which shows maximum value just over 200mT to 80mT at higher distances.
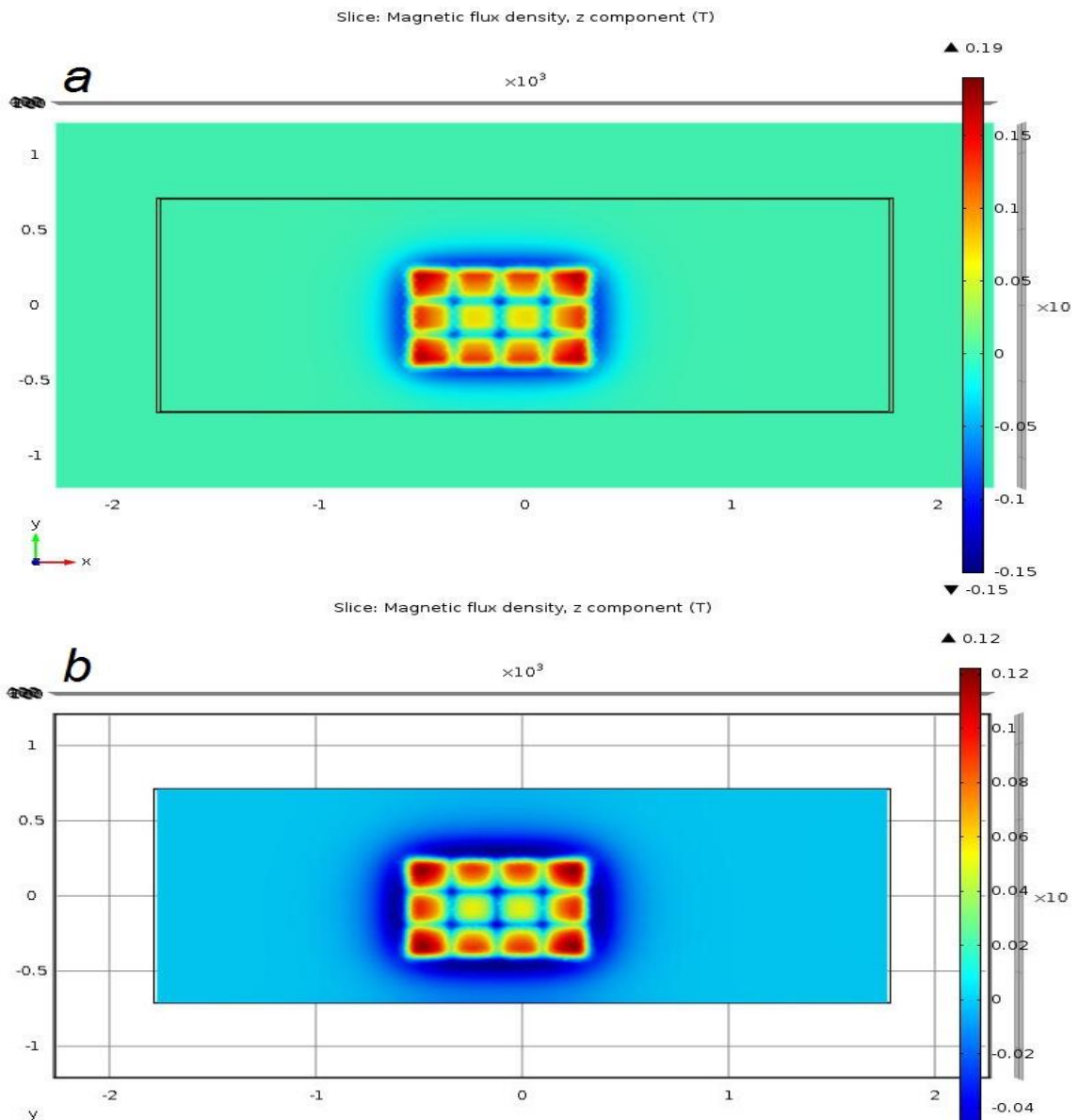

Figure 4.3 z-component of Magnetic flux density (B$_z$) in XY planes, plotted at a) 20μm and b) 40μm above 4 X 3 pattern magnets each 20μm apart with Z-directional magnetization.
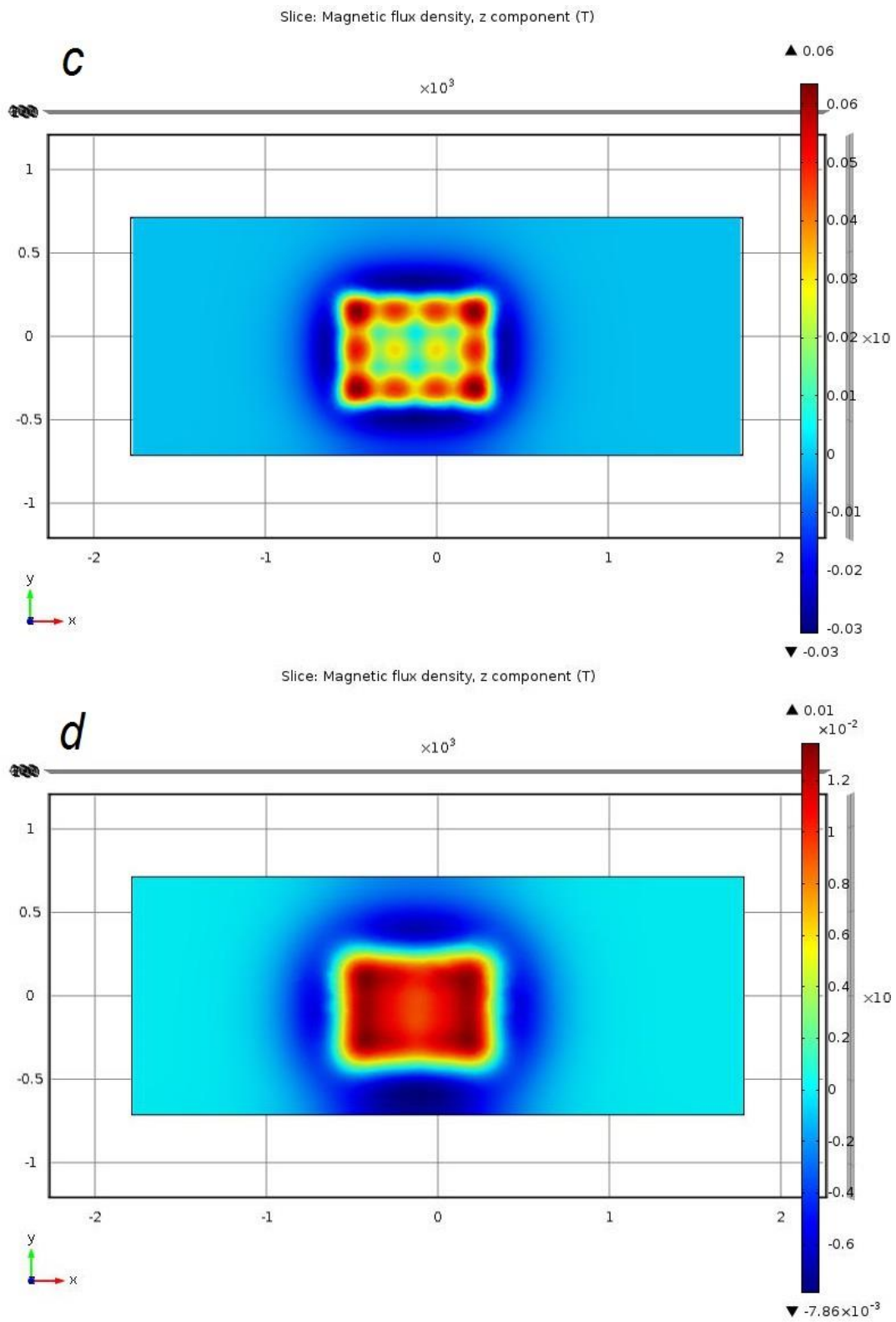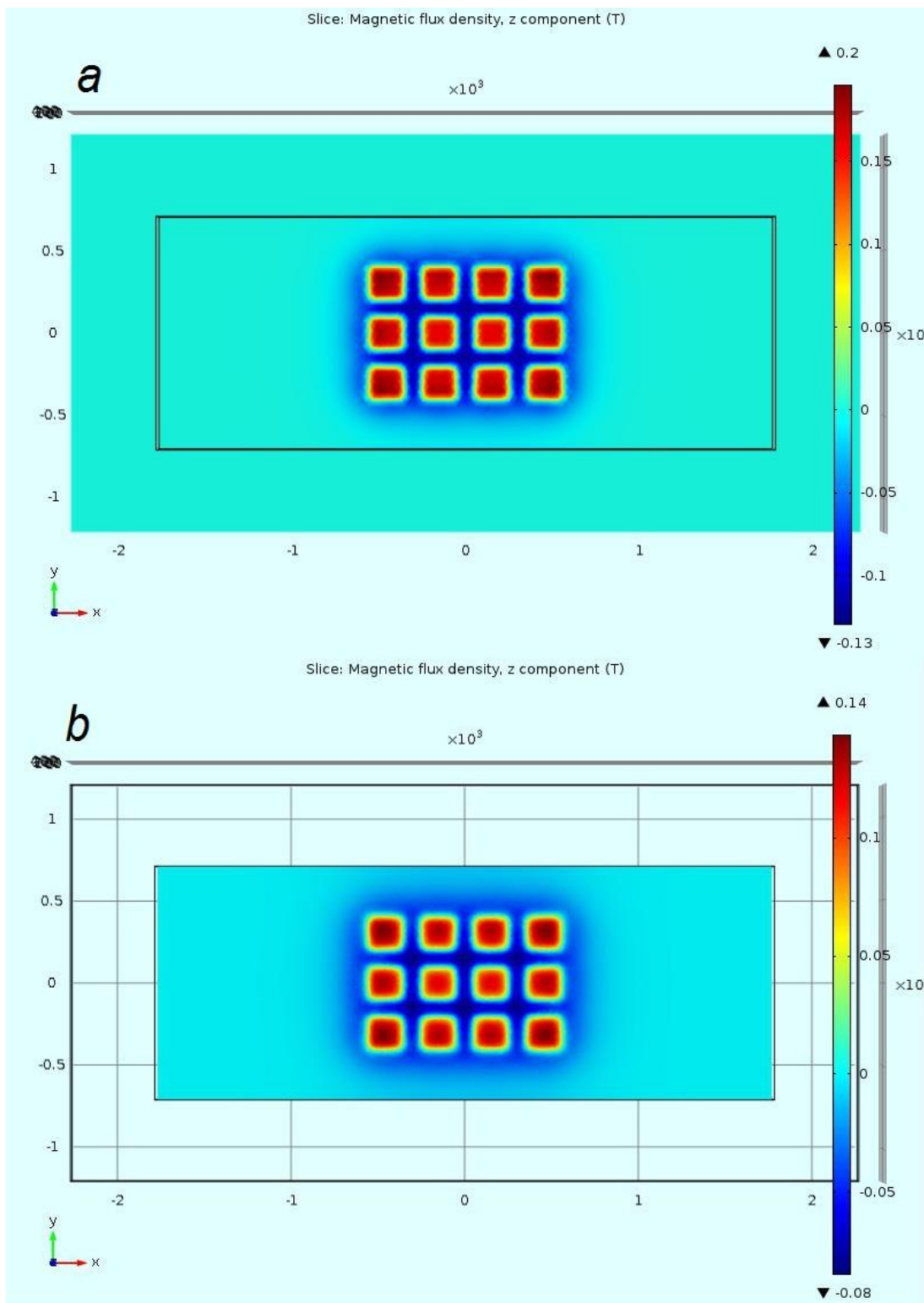
Figure 4.3 z-component of Magnetic flux density (B$_z$) in XY planes, plotted at c) 80µm and d)200µm above 4 X 3 pattern magnets each 20µm apart with Z-directional magnetization.

Figure 4.4 z-component of Magnetic flux density (B_z) in XY planes, plotted at a) 20μm and b)40μm above 4 X 3 pattern magnets each 100μm apart with Z-directional magnetization.
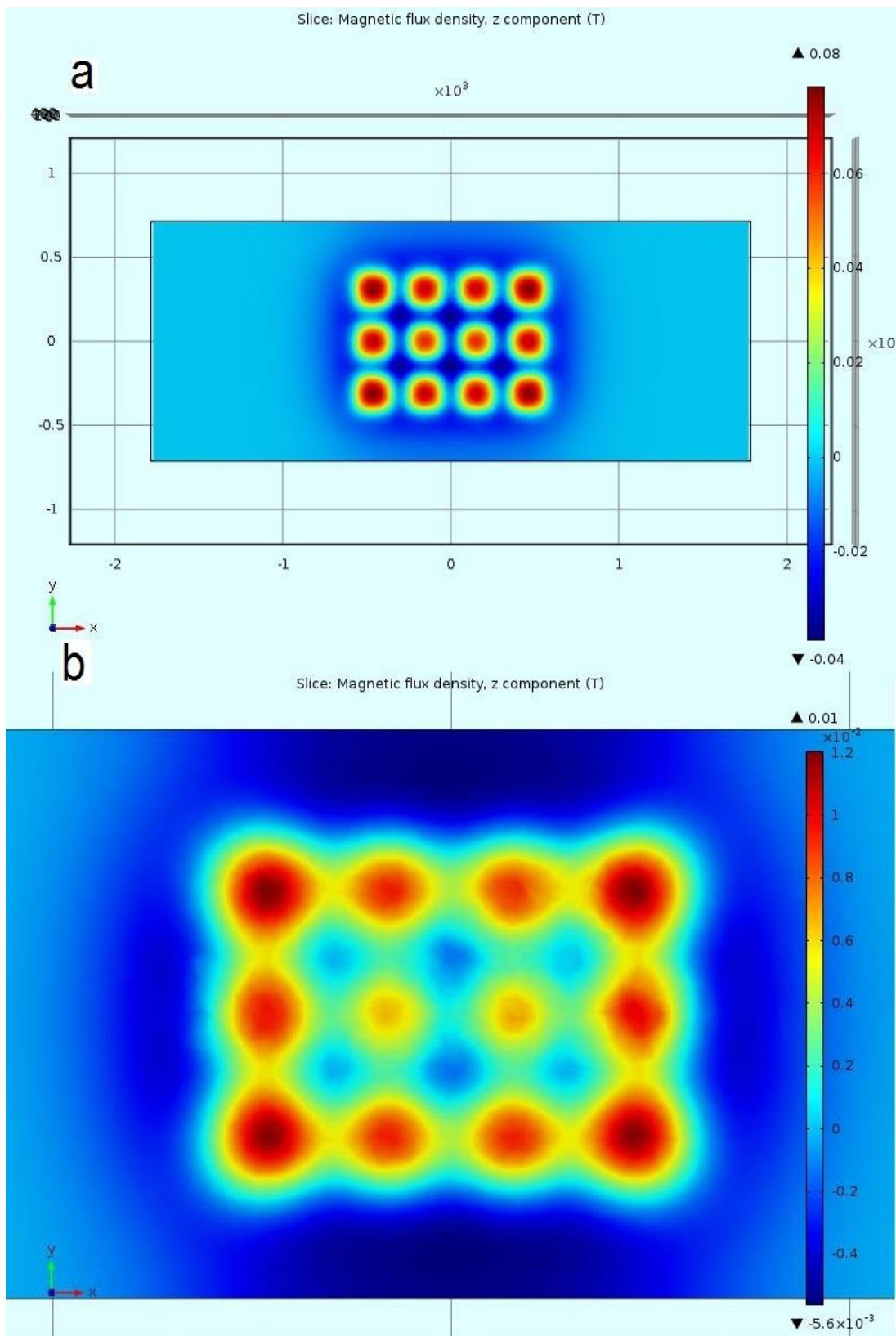
Figure 4.5 z-component of Magnetic flux density (B_z) in XY planes, plotted at a) 80μm and b) 200μm above 4 X 3 pattern magnets each 100μm apart with Z-directional magnetization.

In order to concentrate the cells, we need to trap cells at desired locations which could be achieved using external magnetic force large enough to overcome the hydrodynamic force given by

$$F_h = 6\pi\mu a u$$

We calculated values for F_h in this case with 0.6μm cell radius is found to be 1.1pN. Hence, applied magnetic force F_{mz} must be greater than 1.1pN in order to concentrate the particles efficiently.

In single magnet patterned, at 20μm above the magnet calculated force was seen to be varying in the range of a few nN - few pN as shown in Fig. 4.6. Surprisingly these forces were maximum at the edges near lateral endings compared to the field which was maximum at the center above magnet. The trend of force distribution changes as the height at which the force calculated is increased, showing maximum force field near central area above magnet, which diminishes towards lateral ends. The forces observed were large enough to trap and concentrate the cells above magnet since the minimum force that was observed at heights close to the channel height is 9 pN, very close to F_h.

Similarly, with a pattern of 2 X 2 magnet force can be seen to be more near edges of the array while at the center of pattern, it reduces to have a minima that may levitate particles. But as the distance is increased, we observed that the force due to combined effect of the magnets gives maxima at the center as shown in Fig. 4.7c). The forces were recorded to be varying between 2nN to 8pN throughout the channel.

With 4 X 3 magnetic pattern it can be clearly conferred that increasing number of magnets show a positive effect on field generation. This results in a pattern such that even at heights close to the height of channel, forces can be found to be in tens of pN- large enough to concentrate the particles. Figure 4.8 and Fig. 4.9, show the effect of the force to enable the concentration/aggregation of cells at the center above individual magnet even if the distance from the magnet is high. This effect was exclusively seen in 4 X 3 pattern whereas the minimum field in the spaces between magnets will allow aggregates to be isolated from each other and grow independently.
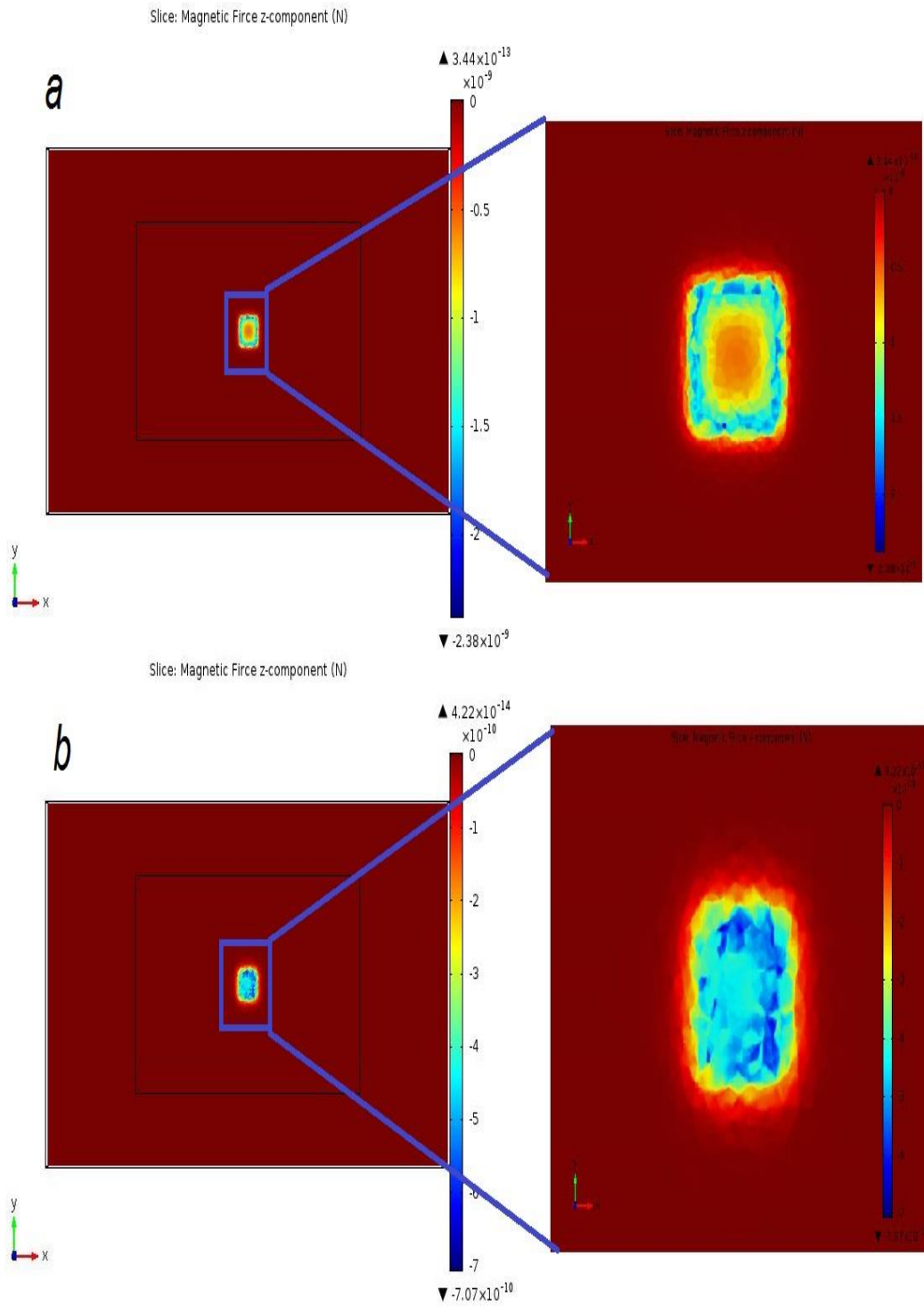
Figure 4.6 z-component of Magnetic Force (F_m) in XY planes, plotted at a) 20 and b) 40µm above magnet in single magnet pattern with Z-directional magnetization. Images on the right hand side shows respective zoom in on the field in Newton.
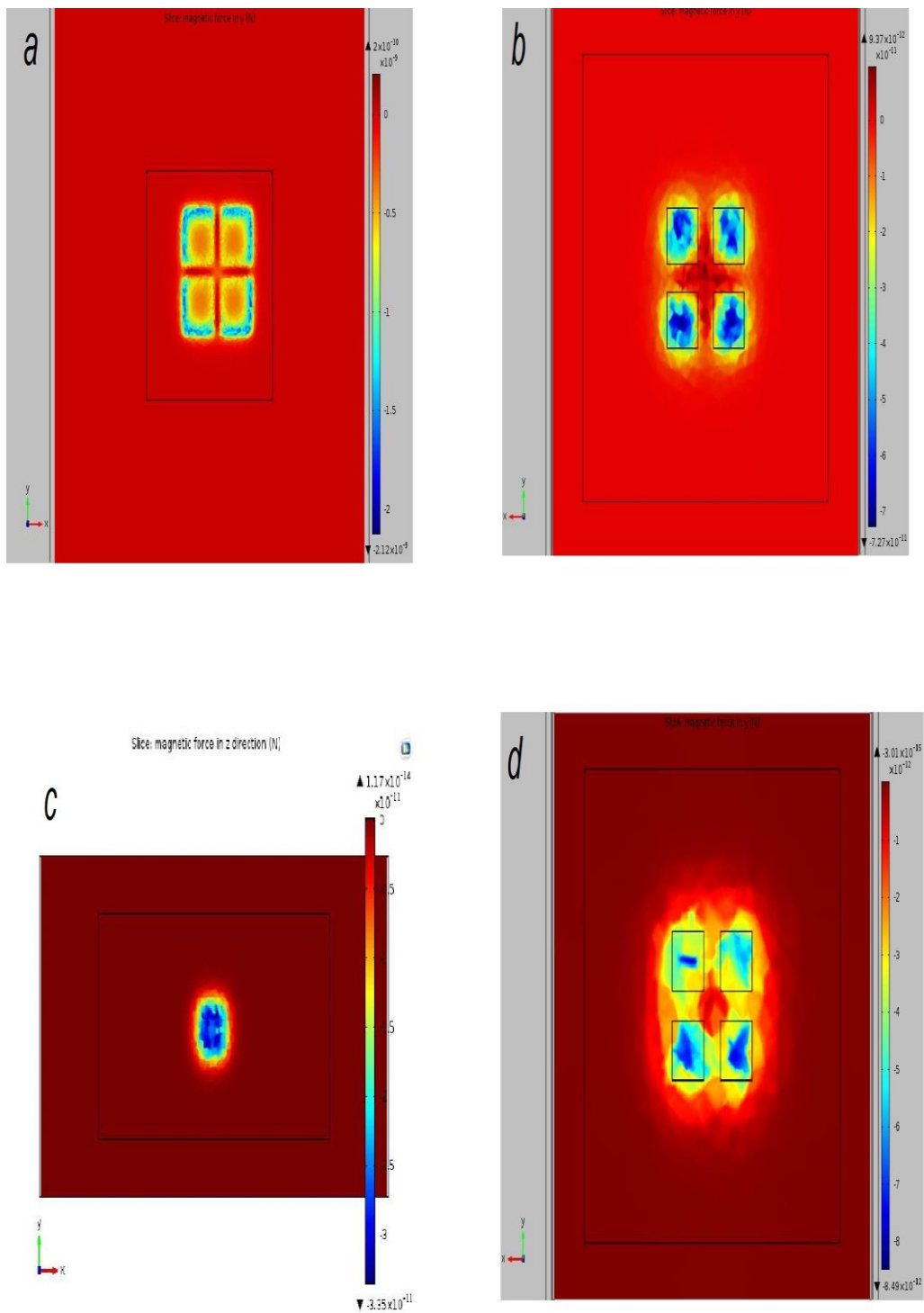
Figure 4.7 z-component of Magnetic Force (F_m) in XY planes, plotted at a) 20, b) 40, c)80 and d) 200μm above 2 X 2 magnetic pattern having 20μm distance between magnets with Z-directional magnetization.
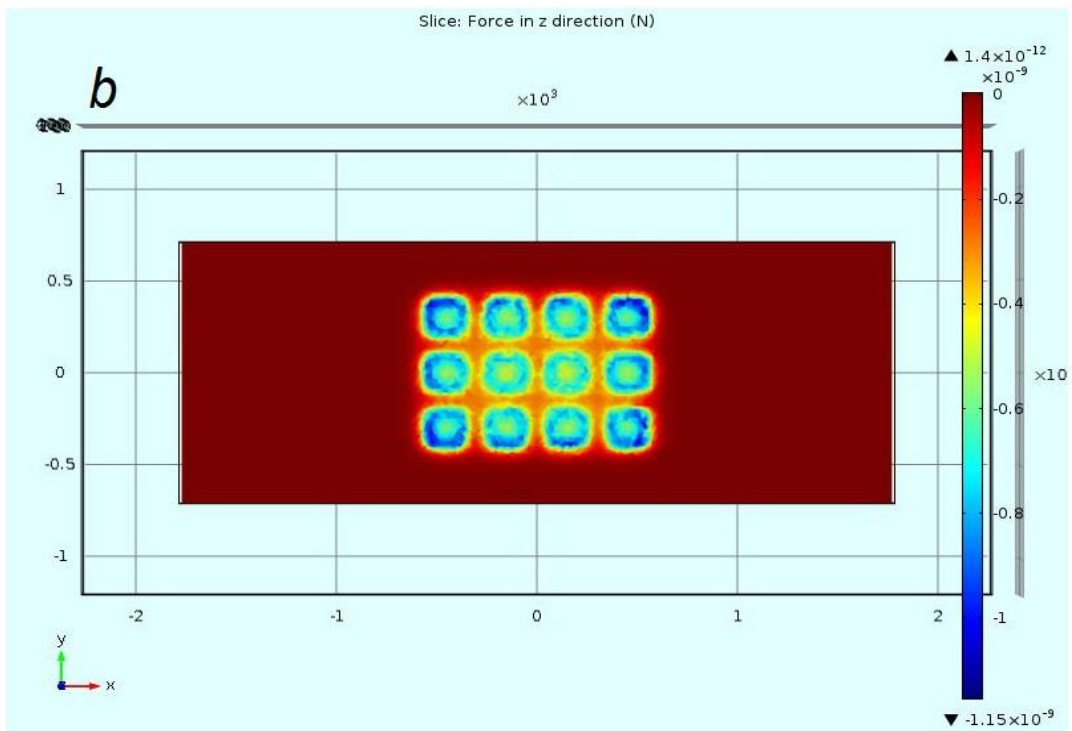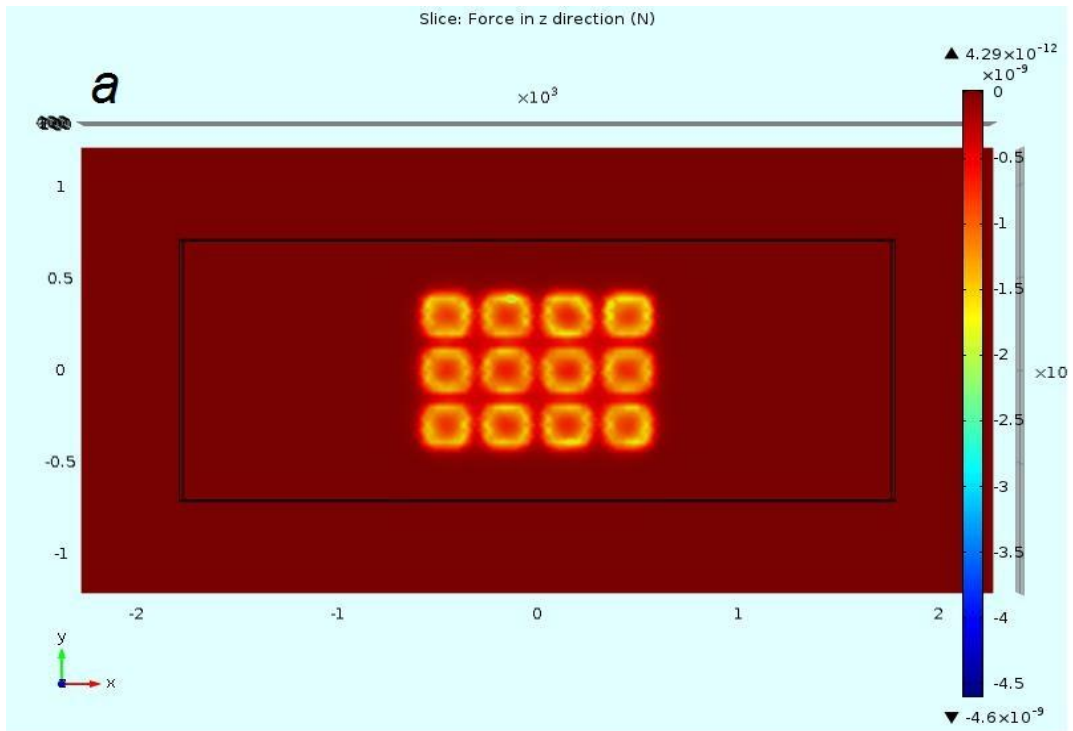
44

Figure 4.8 z-component of Magnetic Force (F_m) in XY planes, plotted at a)20 and b) 40µm above 4 X 3 magnetic pattern with Z-directional magnetization. This force fields are seen to be concentrated on centers above individual magnets, hence can facilitate aggregate isolation and growth without mutual interference.

Figure 4.9 z-component of Magnetic Force (F_m) in XY planes, plotted at a)80 and b) 200µm above 4 X 3 magnetic pattern with Z-directional magnetization. This force fields are seen to be concentrated on centers above individual magnets, hence can facilitate aggregate isolation and growth without mutual interference.
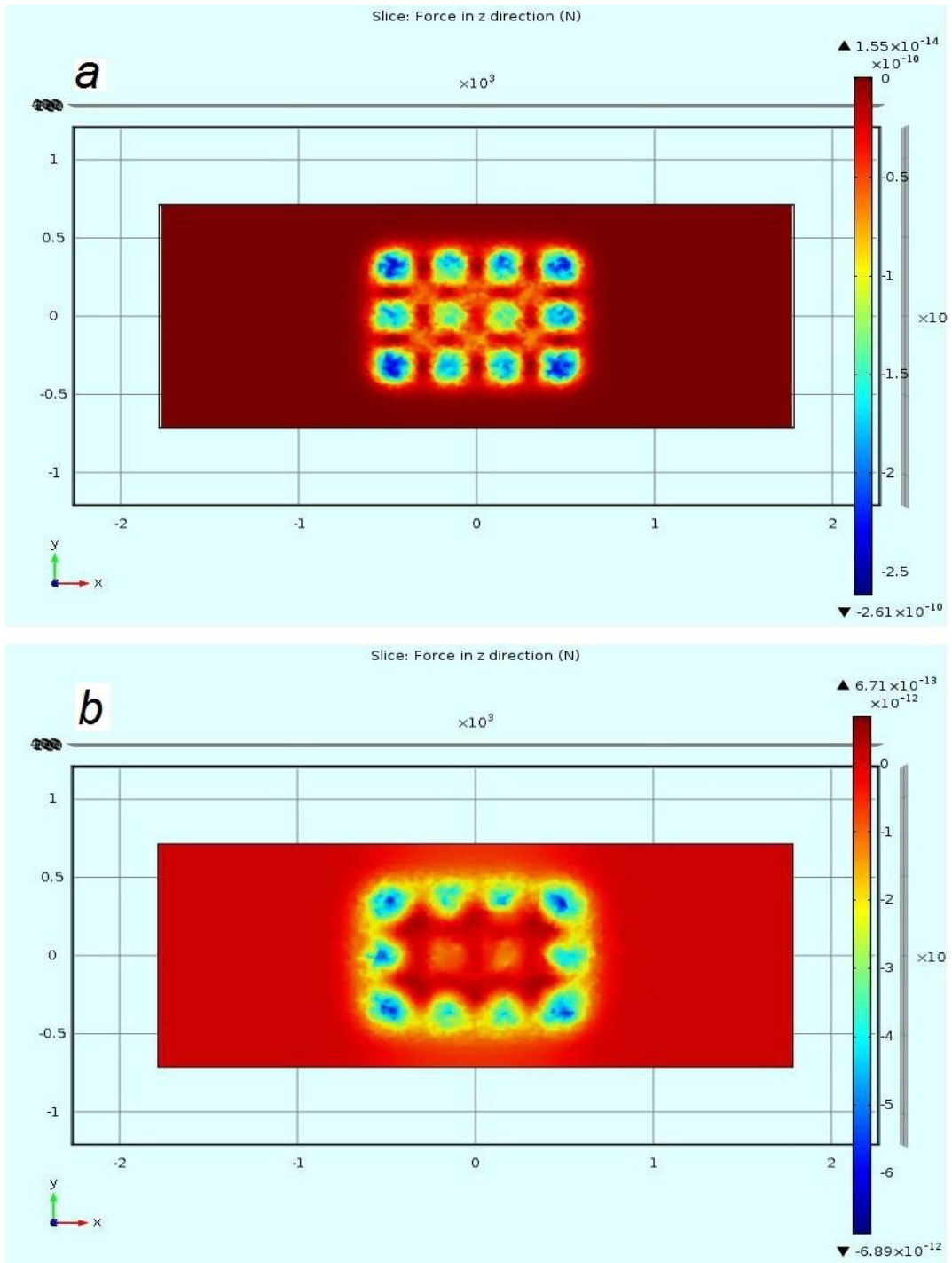
Velocity profiles were studied that was expected to be parabolic in nature due to laminar flow and Newtonian fluid in the direction of the flow. Observed velocity in y-z plane shows elliptical nature due to expression of velocity variation in z and y direction as shown in Fig. 4.10. Above calculations of force fields and velocity fields give enough evidence that, stem cells which are imbibed with magMP will be able to form aggregates or EBs at the locations that show greater magnetic force than hydrodynamic force. This concentration of cells can be observed in Fig. 4.11, which shows normalized concentration variation in X and Y directions when plotted at a height of 100µm above magnet. It can be conferred that concentration is higher close to magnets and is maximum at the center above magnet, and slightly reduces towards distal ends.

Thus, this model of the microfluidic device can be translated into fabrication to validate the proposed simulated studies. The aggregation of cells will lead to differentiation which can be studied further for developmental application. In this study we used permanent microfabricated magnets which restricts the application of device to studying cell culture of differentiation only. However, this method doesn't allow passaging and transfer of cell aggregates to other standard culture environments. Thus, another approach that can be feasible for allowing control over passaging is presumed to be with the use of electromagnets, although care has to be taken for maintaining cell viability and avoiding heating effects.

In future, using more sophisticated techniques of fabrication and advance magnetic research, magnetic field gradients can also be used for enabling control over passage. It is foreseen that magnetic susceptibility in medium can be induced instead of cells which can reduce complexities involved in the process of magMP incorporation in cells.

To conclude the study, we constructed a model to aggregate and manipulate stem cells incorporated with magMP using micropatterned microfabricated magnets in a microfluidics device. This study of aggregation will be helpful in studying differentiation and signaling mechanisms of stem cells. In future it can assist in in addressing challenging questions in the field developmental biology, stem cell research, and scaffold free tissue engineering and regenerative medicine.
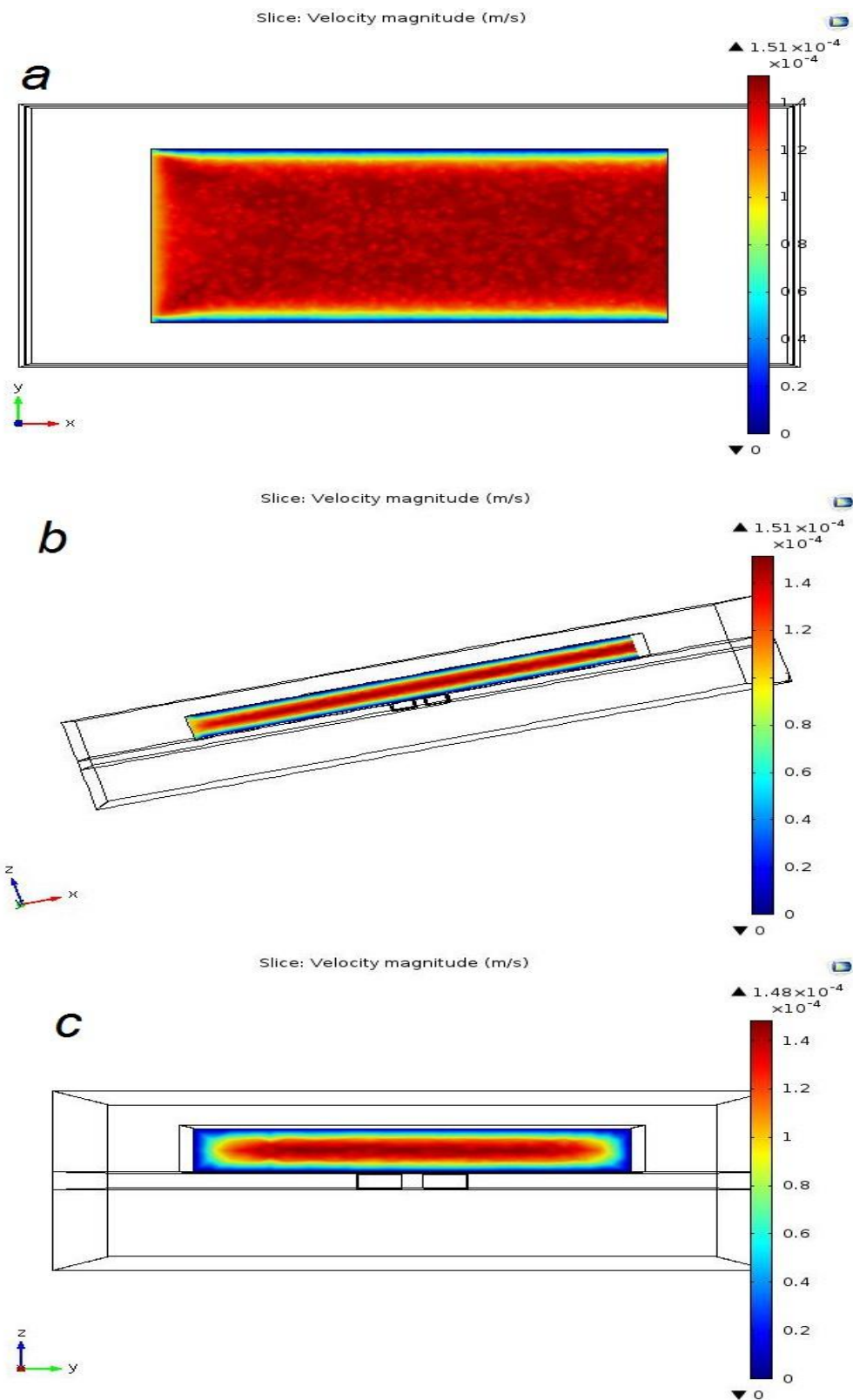
Figure 4.10 Velocity field at the center of channel in a) XY plane, b) XZ plane and c) YZ plane at steady-state flow.
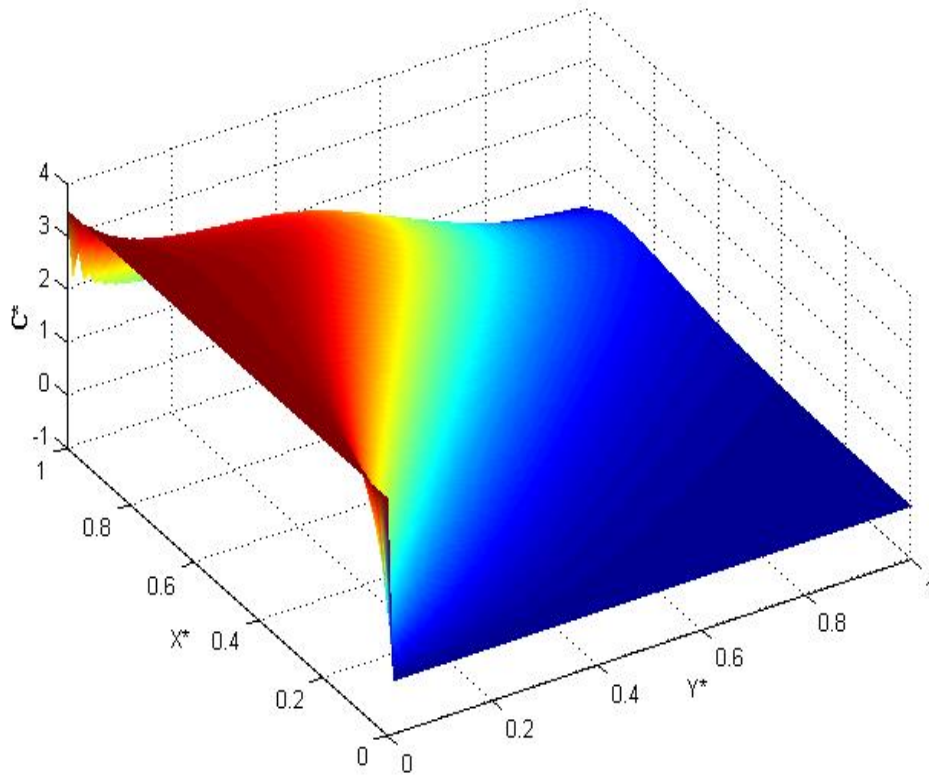
Figure 4.11 Normalized concentration (c*) distribution varying with variation in x and y directions, plotted at 100μm above magnet. At larger heights, concentration reduces to reach a value 1.

Chapter 5

Tables

Table 5.1 Basic properties of materials used in simulations

Material Property	Value (Unit)
Density of DI water	1060 (kg/m^3)
Dynamic viscosity of water	1x10^{-3} (Pa-s)
Relative permeability of water	1
Density of PDMS	970 (kg/m^3)
Relative permeability of PDMS	2.75
Relative permeability of NdFeB magnet	4000
Magnetization in magnets in z and x-directions	800 (kA/m)
Relative permeability of glass	1
Density of glass	2210 (kg/m^3)
Magnetic Susceptibility of water (χ_m)	-0.719x10^{-6}
Magnetic Susceptibility of magnetic microparticles (χ_p)	1
Radius of magnetic microparticle (a)	0.6 (μm)

References

[1]   R. E. Schwartz, H. E. Fleming, S. R. Khetani, and S. N. Bhatia, "Pluripotent stem cell-derived hepatocyte-like cells.," *Biotechnol. Adv.*, vol. 32, no. 2, pp. 504–13, Jan. 2014.

[2]   J. A. Thomson, "Embryonic Stem Cell Lines Derived from Human Blastocysts," *Science (80-.).*, vol. 282, no. 5391, pp. 1145–1147, Nov. 1998.

[3]   J. Itskovitz-Eldor, M. Schuldiner, D. Karsenti, a Eden, O. Yanuka, M. Amit, H. Soreq, and N. Benvenisty, "Differentiation of human embryonic stem cells into embryoid bodies compromising the three embryonic germ layers.," *Mol. Med.*, vol. 6, no. 2, pp. 88–95, 2000.

[4]   E. S. Ng, R. P. Davis, L. Azzola, E. G. Stanley, and A. G. Elefanty, "Forced aggregation of defined numbers of human embryonic stem cells into embryoid bodies fosters robust, reproducible hematopoietic differentiation," *Blood*, vol. 106, no. 5, pp. 1601–1603, 2005.

[5]   J. C. Mohr, J. J. de Pablo, and S. P. Palecek, "3-D microwell culture of human embryonic stem cells," *Biomaterials*, vol. 27, no. 36, pp. 6032–6042, 2006.

[6]   A. M. Bratt-Leal, K. L. Kepple, R. L. Carpenedo, M. T. Cooke, and T. C. McDevitt, "Magnetic manipulation and spatial patterning of multi-cellular stem cell aggregates," *Integr. Biol.*, vol. 3, no. 12, p. 1224, 2011.

[7]   T. Isscr, "Stem Cell Facts," pp. 1–8, 2011.

[8]   S. C. Basics, "Stem cell information," pp. 1–2, 2013.

[9]   P. Ertl, D. Sticker, V. Charwat, C. Kasper, and G. Lepperdinger, "Lab-on-a-chip technologies for stem cell analysis," *Trends Biotechnol.*, vol. 32, no. 5, pp. 245–253, 2014.

[10]   G. M. Whitesides, "The origins and the future of microfluidics.," *Nature*, vol. 442, no. 7101, pp. 368–73, Jul. 2006.

[11]   D. Van Noort and S. M. Ong, "Stem Cells in Microfluidics," 2009.

[12]   D. N. Breslauer, P. J. Lee, and L. P. Lee, "Microfluidics-based systems biology.," *Mol. Biosyst.*, vol. 2, no. 2, pp. 97–112, Feb. 2006.

[13]   S. Zheng, H. Lin, J. Q. Liu, M. Balic, R. Datar, R. J. Cote, and Y. C. Tai, "Membrane microfilter device for selective capture, electrolysis and genomic

analysis of human circulating tumor cells," *J. Chromatogr. A*, vol. 1162, no. 2 SPEC. ISS., pp. 154–161, 2007.

[14] D. Di Carlo, N. Aghdam, and L. P. Lee, "Single-cell enzyme concentrations, kinetics, and inhibition analysis using high-density hydrodynamic cell isolation arrays.," *Anal. Chem.*, vol. 78, no. 14, pp. 4925–30, Jul. 2006.

[15] A. M. Skelley, O. Kirak, H. Suh, R. Jaenisch, and J. Voldman, "Microfluidic control of cell pairing and fusion.," *Nat. Methods*, vol. 6, no. 2, pp. 147–52, Feb. 2009.

[16] H. A. Pohl and K. Pollock, "Electrode geometries for various dielectrophoretic force laws," *J. Electrostat.*, vol. 5, pp. 337–342, Sep. 1978.

[17] M. Toner and D. Irimia, "Blood-on-a-chip.," *Annu. Rev. Biomed. Eng.*, vol. 7, pp. 77–103, Jan. 2005.

[18] M. a M. Gijs, "Magnetic bead handling on-chip: New opportunities for analytical applications," *Microfluid. Nanofluidics*, vol. 1, no. 1, pp. 22–40, 2004.

[19] N. Pamme, "Magnetism and microfluidics.," *Lab Chip*, vol. 6, no. 1, pp. 24–38, 2006.

[20] Z. J. Gartner and C. R. Bertozzi, "Programmed assembly of 3-dimensional microtissues with defined cellular connectivity.," *Proc. Natl. Acad. Sci. U. S. A.*, vol. 106, no. 12, pp. 4606–4610, 2009.

[21] M. P. Lutolf and J. A. Hubbell, "Synthetic biomaterials as instructive extracellular microenvironments for morphogenesis in tissue engineering.," *Nat. Biotechnol.*, vol. 23, no. 1, pp. 47–55, Jan. 2005.

[22] D. R. Albrecht, G. H. Underhill, T. B. Wassermann, R. L. Sah, and S. N. Bhatia, "Probing the role of multicellular organization in three-dimensional microenvironments.," *Nat. Methods*, vol. 3, no. 5, pp. 369–75, May 2006.

[23] R. Gauvin and A. Khademhosseini, "Microscale technologies and modular approaches for tissue engineering: moving toward the fabrication of complex functional structures.," *ACS Nano*, vol. 5, no. 6, pp. 4258–64, Jun. 2011.

[24] D. Falconnet, G. Csucs, H. M. Grandin, and M. Textor, "Surface engineering approaches to micropattern surfaces for cell-based assays.," *Biomaterials*, vol. 27, no. 16, pp. 3044–63, Jun. 2006.

[25] C. Xu, M. S. Inokuma, J. Denham, K. Golds, P. Kundu, J. D. Gold, and M. K. Carpenter, "Feeder-free growth of undifferentiated human embryonic stem cells.," *Nat. Biotechnol.*, vol. 19, no. 10, pp. 971–4, Oct. 2001.

[26] S. Han, K. Yang, Y. Shin, J. S. Lee, R. D. Kamm, S. Chung, and S.-W. Cho, "Three-dimensional extracellular matrix-mediated neural stem cell differentiation in a microfluidic device," *Lab Chip*, vol. 12, no. 13, p. 2305, 2012.

[27] C. L. Bauwens, R. Peerani, S. Niebruegge, K. a Woodhouse, E. Kumacheva, M. Husain, and P. W. Zandstra, "Control of human embryonic stem cell colony and aggregate size heterogeneity influences differentiation trajectories.," *Stem Cells*, vol. 26, no. 9, pp. 2300–2310, 2008.

[28] S. J. Morrison, M. Csete, A. K. Groves, W. Melega, B. Wold, and D. J. Anderson, "Culture in reduced levels of oxygen promotes clonogenic sympathoadrenal differentiation by isolated neural crest stem cells.," *J. Neurosci.*, vol. 20, no. 19, pp. 7370–6, Oct. 2000.

[29] M. Khoury, A. Bransky, N. Korin, L. C. Konak, G. Enikolopov, I. Tzchori, and S. Levenberg, "A microfluidic traps system supporting prolonged culture of human embryonic stem cells aggregates," *Biomed. Microdevices*, vol. 12, no. 6, pp. 1001–1008, 2010.

[30] M. Navab, S. S. Imes, S. Y. Hama, G. P. Hough, L. A. Ross, R. W. Bork, A. J. Valente, J. A. Berliner, D. C. Drinkwater, and H. Laks, "Monocyte transmigration induced by modification of low density lipoprotein in cocultures of human aortic wall cells is due to induction of monocyte chemotactic protein 1 synthesis and is abolished by high density lipoprotein.," *J. Clin. Invest.*, vol. 88, no. 6, pp. 2039–46, Dec. 1991.

[31] A. Revzin, R. G. Tompkins, and M. Toner, "Surface Engineering with Poly(ethylene glycol) Photolithography to Create High-Density Cell Arrays on Glass," *Langmuir*, vol. 19, no. 23, pp. 9855–9862, Nov. 2003.

[32] A. Manuscript, "NIH Public Access," *Changes*, vol. 29, no. 6, pp. 997–1003, 2012.

[33] R. Langer and J. P. Vacanti, "Tissue engineering.," *Science*, vol. 260, no. 5110, pp. 920–6, May 1993.

[34] S. Khetan and J. A. Burdick, "Patterning network structure to spatially control cellular remodeling and stem cell fate within 3-dimensional hydrogels.," *Biomaterials*, vol. 31, no. 32, pp. 8228–34, Nov. 2010.

[35] N. Pamme, J. C. T. Eijkel, and A. Manz, "On-chip free-flow magnetophoresis: Separation and detection of mixtures of magnetic particles in continuous flow," *J. Magn. Magn. Mater.*, vol. 307, no. 2, pp. 237–244, 2006.

[36] P. Pham, I. Texier, and F. Perraut, "From Numerical to Experimental Study of Microsystems for Dielectrophoresis on Bioparticles," *Comsol Conf. Paris*, pp. 1–8, 2006.

[37] F. Sarreshtedari, H. Kokabi, and J. Gamby, "AGGREGATION AND DETECTION OF MAGNETIC NANOPARTICLES IN MICROFLUIDIC CHANNELS," vol. 63, no. 7, pp. 27–30, 2012.